EUMETSAT/ECMWF Fellowship Programme,
Research Report No. 14

Assimilation of Geostationary WV Radiances from GOES and Meteosat at ECMWF

Christina Köpken, Jean-Noël Thépaut, and Graeme Kelly

April 2003

For additional copies please contact

The Library
ECMWF
Shinfield Park
Reading
RG2 9AX
library@ecmwf.int

Series: EUMETSAT/ECMWF Fellowship Program - Research Reports

A full list of ECMWF Publications can be found on our web site under:
http://www.ecmwf.int/publications/

Abstract

This report describes the current status of geostationary water vapour radiance assimilation in the ECMWF 4DVAR system. In addition to the Meteosat–7 data, the operational assimilation of water vapour clear–sky radiances (WV CSR) has been extended to include CSR also from GOES–8 and GOES–10 satellites since 14 January 2003. The GOES CSR data product is described and results from its pre–operational monitoring are discussed. Small, but regular bias changes occur around local midnight and are probably linked to a calibration anomaly. Data selection criteria are introduced to exclude possibly affected data and to reduce cloud contamination. Assimilation experiments have been carried out and show a similar influence of the data as was obtained with Meteosat–7 data. The most prominent systematic change is a reduction of upper tropospheric humidity in the inner tropical convergence zone while humidity increases in adjacent areas. This is in accordance with HIRS observations and leads to a better fit of the model first guess with these radiances. Also, in some periods and areas, the first guess fit of conventional upper level wind and humidity observations is improved. The impact on forecast quality is slightly positive to neutral for different areas of the globe, the positive impact being found mostly in the upper level fields (around 200 hPa).
For the Meteosat CSR, an update of monitoring results is given and the influence of the orbit position variations of Meteosat–5 in the CSR is described. CSR from the reprocessed Meteosat–2 data have been monitored within the ERA–40 reanalysis. Results show that despite the lower bit representation of the image data in the WV channel, the Meteosat–2 CSR are approximately comparable to those of Meteosat–7 in terms of fit to the model first guess. However, there is an indication for a higher cloud contamination present in the CSR. Also, the calibration, based on the vicarious method is not stable enough for a direct assimilation of the data.

1 Introduction

The fellowship was directed at investigating the use of observations of geostationary platforms in the form of direct radiance assimilation within a 4–DVAR framework continuing the work started by Munro et al. (1999). While the direct assimilation of radiances from sounding instruments on polar orbiting satellites is well established (e.g. Andersson et al., 1994; McNally et al., 2000), data from geostationary imagers have primarily been used for operational numerical weather prediction (NWP) either in the form of atmospheric motion vectors (AMV) derived from tracking features in the imagery or in the form of cloud top information (e.g. MacPherson et al., 1996). Compared to radiance observations from polar orbiting satellites, data from geostationary platforms offer a considerably higher time resolution and therefore a quasi–continuous description of, e.g. the water vapour field in the high troposphere. Within a 4DVAR assimilation system, this allows tracking of the observed movement of humidity structures and thereby derivation of corrections to the wind field together with corrections to humidity (and temperature). Compared to the current usage of clear–sky AMVs for which the height assignment is particularly problematic, this approach has the advantage that the depth of the layer emitting the radiation is directly taken into account through the radiative transfer (RT) calculations.

Currently, the imager data are used in the form of area averaged clear–sky radiances (CSR) which are derived by EUMETSAT (European Organization for the Exploitation of Meteorological Satellites, Germany) for the Meteosat satellites, and by the Cooperative Institute for Meteorological Satellite Studies (CIMSS, USA) for the GOES satellites. The WV CSR (or brightness temperatures, TB) of Meteosat–7, GOES–8, GOES–10 are assimilated operationally (see Figure 1), and Meteosat–5 is passively monitored. Global coverage may be achieved in spring 2003 when GOES–9 will replace the Japanese GMS satellite and provide observations over the Pacific.

The work during the fellowship has covered the following main areas:

- Monitoring of water vapour and infrared clear–sky radiances of Meteosat–7 and Meteosat–5, concentrating particularly on quality issues that became apparent in the comparisons to the model first guess:
  - Characterization of solar stray light effects in Meteosat radiances throughout the year based on two years of monitoring.

  - Monitoring of biases in the water vapour and infrared channels.
  - Cross comparisons with similar channels on other polar–orbiting and geostationary satellites (NOAA/HIRS, NOAA/AMSUB, GOES).
  - Characterization of biases in Meteosat–5 radiances linked to the variation of the satellite inclination around its nominal position.

- Assimilation experiments using Meteosat–7 and implementation into operational assimilation on 9 April 2002.
- Liasing with CIMSS/NESDIS for the development of a clear–sky radiance product from GOES imagers and implementation and monitoring of GOES–8 and GOES–10 CSR within the ECMWF system.
- Assimilation experiments using GOES–8 and GOES–10 WV radiances and implementation of the assimilation into operations on 14 January 2003.
- Assimilation experiments with a new formulation of humidity analysis.
- Development and implementation of a new monitoring package enabling a wider range of monitoring statistics and the monitoring of different satellites within the same framework (preparation for the monitoring of MSG).
- Automization of the bias correction programs for use in operations
- Preparation of the assimilation system to accomodate additional GOES satellites and MSG.
- Implementation of processing of early Meteosat satellites (Meteosat–1 to Meteosat–4) and monitoring of reprocessed data of Meteosat–2 within the ERA–40 reanalysis.

This report concentrates primarily on the clear–sky radiances of GOES satellites, their monitoring (Section 2), and their implementation into operational assimilation (Section 3) as well as tests with the new formulation of the humidity analysis (Section 4). However, it also includes an update of the monitoring results of Meteosat

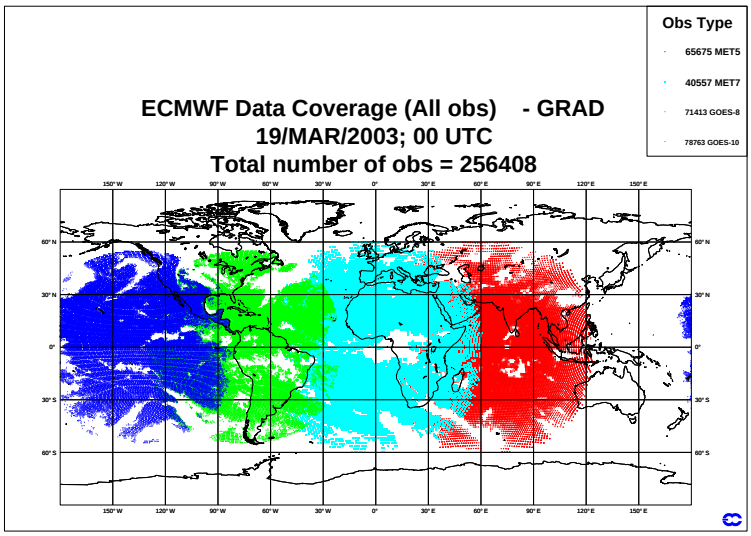

Figure 1: Example of operational data coverage with geostationary clear–sky radiances over a 6 hour window. Meteosat–7 (light blue), GOES–8 (green), and GOES–10 (dark blue) are operationally assimilated. Meteosat–5 (red) is passively monitored.

radiances, in particular Meteosat–5. A description of the preparations done in view of MSG data is also given in Section 2. Section 5 adds an initial assessment of the quality of the reprocessed Meteosat–2 data from their monitoring in the ERA reanalysis. A summary of the status of geostationary radiance usage at ECMWF and possible future areas of work is given in Section 6.
Results obtained during this fellowship and summarized in this report as well as in the two previous ones, Köpken (2001) and Köpken et al. (2002), have been presented at the EUMETSAT User's conference 2001, the ITSC conference 2002, the ECMWF workshop on humidity analysis 2002, and the 12th AMS conference on satellite meteorology and oceanography, 2003. They have also been submitted for publication as Köpken (2003), Munro et al. (2003), and Köpken et al. (2003).

2 Clear–sky radiances from GOES and Meteosat

2.1 Clear–sky radiances from GOES–8 and GOES–10

Following the experience with the CSR from the Meteosat and its positive impact in assimilation, the derivation of a similar product from other geostationary satellites was initiated. Subsequently, since 24 October 2001, clear–sky radiances have been produced for the GOES imagers by the Cooperative Institute for Meteorological Satellite Studies (CIMSS, Madison, USA). Following initial monitoring and assimilation experiments, the WV channel CSR of both GOES–8 and GOES–10 are operationally assimilated since 14 January 2003.

2.1.1 The clear–sky radiance product from GOES satellites

The GOES CSR data are derived for all 5 channels, the visible (VIS) the 3 infrared window channels (IR) at 3.9 μm, 10.7 μm, 11.9 μm, and the water vapour channel (WV) at 6.7 μm at a resolution of about $45 \cdot 45$ km at SSP. The same cloud mask is applied for all the channels and the percentage of clear and cloudy pixels in each CSR segment are encoded along with the data. Pending full operational implementation at NESDIS (Washington, USA), the BUFR encoded CSR data are received via ftp–transfer from CIMSS. Following feedback from the monitoring at ECMWF and also at NCEP (Washington, USA; Xiujuan Su), the CSR product has been updated several times, mostly on the technical level. The main change in content was the introduction of a tighter cloud detection on 4 September 2002 which has reduced a negative bias in the IR window channels by about 1 K while the WV channel remained nearly unchanged. Since end of 2002, the standard deviation of pixels within the CSR segment has been included as a quality measure. The addition of further quality information is being discussed.

2.1.2 Monitoring and quality issues

The GOES data have been monitored offline from 24 October to end of December 2001 and from then onwards in first the pre–operational and since 9 April 2002 in the operational assimilation system. As for the Meteosat data, the monitoring concentrated on determining biases in the data and detecting possible specific effects, like the stray light intrusions found for the Meteosat measurements. Figure 2 shows as an example time series of mean departures of CSR from the model first guess for the WV CSR of GOES–8 and GOES–10 for the period mid January to mid March 2002. The mean biases of GOES–10 and GOES–8 are about 0.8 K and 1.4 K, respectively, and have overall been very stable. For comparison, Figure 2, shows the monitoring for the WV channel of both Meteosat satellites and the channels 12 on HIRS and 3 on AMSUB for the same period. While the Meteosat satellites have considerably larger departures of about 3 K and 3.8 K for Meteosat–5 and Meteosat–7, respectively (e.g. in March 2002), the humidity sounding channels on the polar orbiters measure slightly colder brightness temperatures than the corresponding model values. The different bias values clearly make a bias

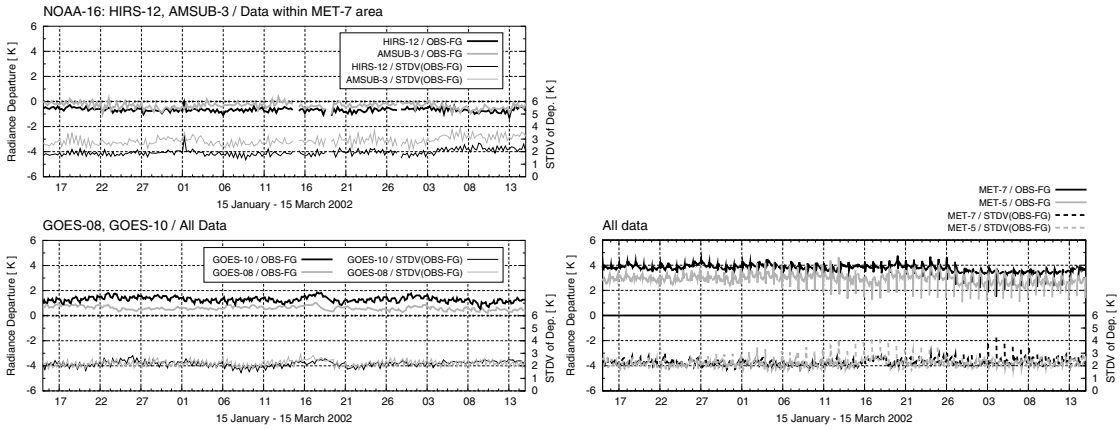

Figure 2: Time series of mean differences between radiance observations and model first guess (as brightness temperatures in K, left axis) and standard deviations of the differences (right axis) for 15 January 2002 until 15 March 2002. Top left : For NOAA–16 HIRS–12 (black curve) and AMSUB–3 (grey curve) data within a square area covering the Meteosat–7 disk. Bottom left: For GOES–08 (grey curve) and GOES–10 (black curve) CSR. Botom right: For Meteosat–7 (black curves) and Meteosat–5 (grey curves) CSR.

correction of all data necessary. In terms of standard deviation, the GOES data have very similar values to the CSR from Meteosat and HIRS (about 2–2.4 K). For the GOES data, small variations in bias do occur. The changes around 17–20 February visible in Figure 2 are caused by HIRS–12 data not having been assimilated for a few days. For many other changes of comparable magnitude (0.5–1 K) seen during the initial months between October 2001 and May 2002, the results of passive data from the corresponding HIRS and AMSUB channels have been inspected. Mostly, similar changes in bias could be found in their monitoring within the respective areas of GOES–8 and GOES–10. Therefore, these changes in bias are attributed to the model first guess rather than to the GOES observations. They may e.g. be caused by the model being insufficiently constrained by observations particularly in the Pacific area.

Contrary to the Meteosat satellites, no particular influence of the solar eclipses are seen in the GOES data. However, there is a striking diurnal variation present in the departures throughout the year for both GOES–8 and GOES–10, but normally stronger for GOES–8 (as visible e.g. in Figure 2). This variation consists in a dip of the biases around local midnight (i.e. 5 UTC and 9 UTC for GOES–8 and GOES–10, respectively). Generally, it is hard to distinguish if the changes in departures result simply from a possible misplacement in time between a modeled and observed true diurnal variation of TBs – or if it is an artifact related to the observations. However, if it is a true phenomenon, both satellites GOES–8 and GOES–10 should observe it in a similar way. Therefore, Figure 3 displays time series of observations, first guess and departures within an area in the overlap between the two satellites. The characteristic 'dips' are visible particularly in the GOES–8 data around 5 UTC. This becomes even more distinct when looking at the difference plot in the bottom panel. This finding suggests that the reduced departures around local midnight are indeed to be attributed to the observations rather than to the model.

Johnson and Weinreb (1996) discuss a study of a calibration anomaly for the GOES imagers which probably explains the observations discussed above. They describe systematically too cold calibrations occuring at local midnight especially in the 'short wave' channels 3.9 μm and 6.7 μm, with little effects visible at the longer wavelengths 10.7 μm and 11.9 μm. They show strong correlations between the measured temperature of especially the outer optical parts of the satellite and changes in the calibration curves. The suggested physical reason for this calibration anomaly is that the strong heating of the parts of the satellite oriented towards the sun during local midnight (the satellite is three axis stabilized) causes extra radiation to be emitted which also reaches the internal blackbody. As the blackbody is not totally black, a small portion of that radiation is then

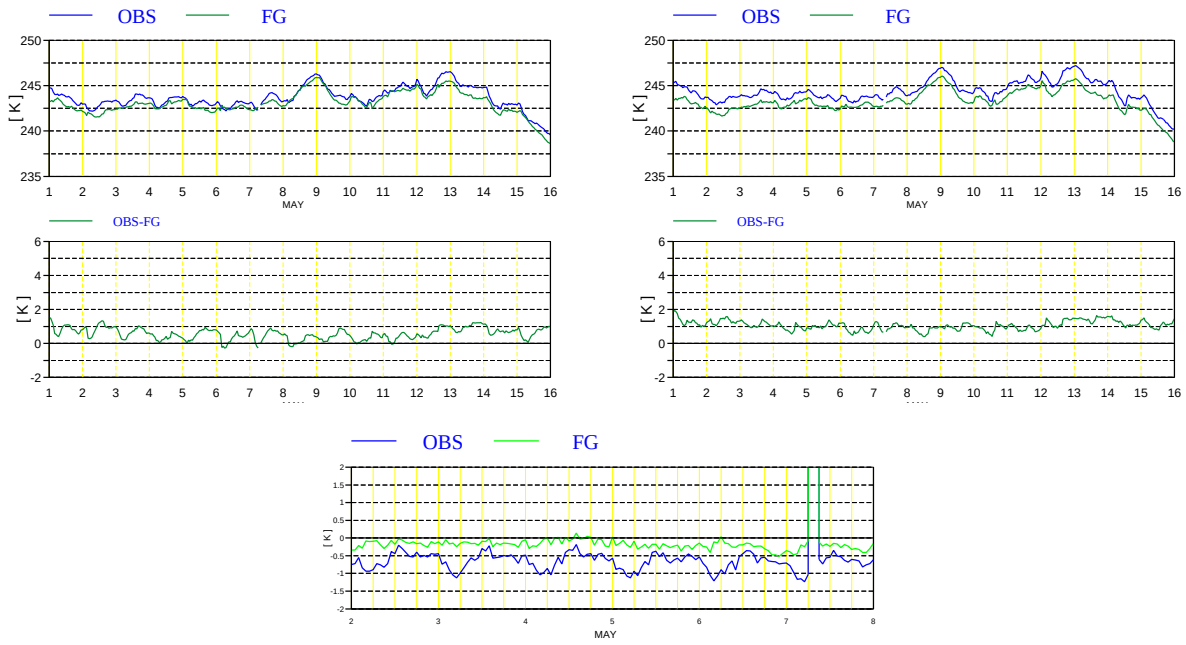

Figure 3: Top panels: Time series of WV channel CSR (blue curves) and corresponding first guess (green curves) for GOES–8 (left) and GOES–10 (right) (as brightness temperatures in K) for a rectangle within the common overlap area (-112° to -102° Lon, 0° to 45° Lat) for 1 to 16 May 2002. Middle panels: As top, but for the first guess departures. Bottom: Difference of observations (blue) and first guesses (green) for GOES–8 minus GOES–10 for 2 to 8 May 2002.

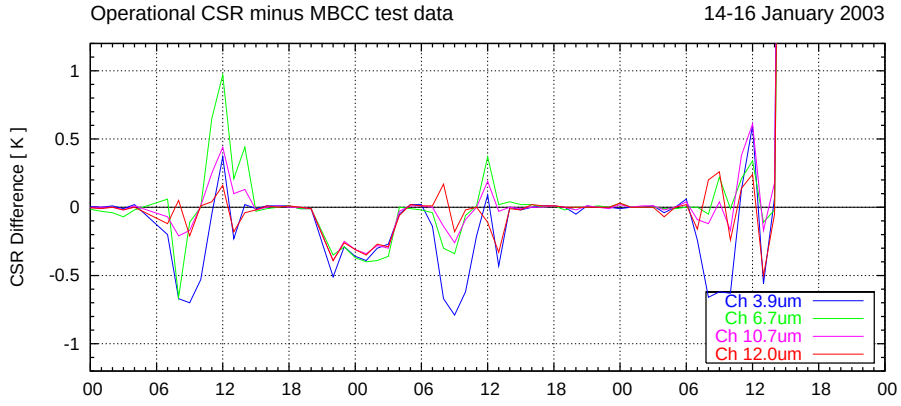

Figure 4: Time series of TB difference (in K) between CSR based on operational data and the GOES–10 test data using the midnight blackbody calibration correction for the 3.9 μm (blue curve), 6.7 μm (green), 10.7 μm (magenta), and 11.9 μm (red). Test data for 14 January 2003 0 UTC until 16 January 2003, 14 UTC.

reflected back but not taken into account in the evaluation of the blackbody view. Due to this, the calibration is affected, especially at shorter wavelengths. The magnitude of the effects, and that it seems to be stronger for GOES–8 than for GOES–10, fits to the diagnostic in the ECMWF monitoring so that the departure changes are believed to be linked to this so–called 'midnight blackbody calibration anomaly'. In difference to the Johnson and Weinreb paper, though, the effect seems to be always present and no very distinct modulation with strongest anomalies during May and July was seen.

After feedback of the results, NOAA (USA) processed three days worth of GOES–10 imager data from 14 to 16 January 2003 using a regression correction to the calibration that was developed based on the correlation between the satellite front optics and the calibration coefficients anomaly. The corresponding CSR data for this test have been compared here versus the first guess and results for the three days are shown in Figure 4. For the 3.9 μm, the test data are indeed warmer by up to 0.7 K at 9 UTC. In the comparison versus the model first guess, the observed minimum disappears as expected. The 6.7 μm WV channel, however, is not systematically warmer between 7 to 11 UTC throughout these three test days, and also the magnitude of the change is smaller than the departure changes in the monitoring, which does therefore not change substantially. Also, the tested regression correction leads to unexpected changes in the longer wavelength split window channels and results in colder than operational TBs (up to 1 K on 14 January for 6.7 μm) at 12 UTC. Associated to these differences are also changes in the number of CSR data received (i.e. changes in the cloud detection at CIMSS). These unexpected differences as well as the changes occuring for all channels around 00 UTC 15 January (Figure 4) are not yet understood by NOAA and an implementation of a correction to the midnight blackbody calibration anomaly is pending awaiting further experimentation.

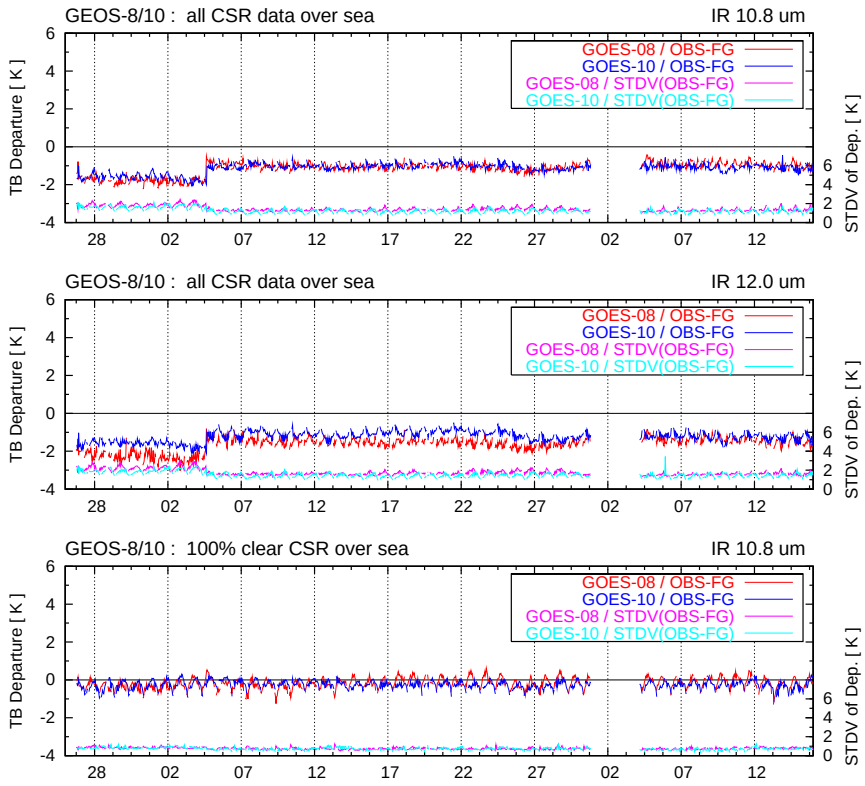

Figure 5: Top: Time series of mean differences between TB (K) of observations and model first guess for the window channels at 10.7 μm together with standard deviations of the differences (right axis) for GOES–8 and GOES–10 for all data over sea during 20 August to 15 October 2002. Middle: As top, but for 11.9 μm. Bottom: as top, but for the CSR with a clear sky fraction of 100%.

From the infrared CSR, particularly the two split window channels are of interest. The 3.9 μm is also being monitored but its solar contribution is not yet modelled by RTTOV and therefore the day time departures are not currently meaningful. Figure 5 shows departure time series for the 10.7 μm and 11.9 μm for mid August to October 2002 over sea. The change in the cloud processing (mainly an improvement in the sea surfcae temperature and related quality control checks) introduced on 4 September 2002 is clearly visible through a reduced bias in both split window channels (while the WV channel bias remained virtually unchanged). Interestingly, the departures for the subset of data having a clear sky fraction of 100% (bottom panel for 10.7 μm) remained unchanged and is only about -0.5 K (for comparison, the bias for observations from HIRS channel 8 is about -1 K, see Figure 10 in Köpken et al., 2002). This points to no (or only very little) cloud contamination present in this data subset. Also, the standard deviation of the departures for this data subset are by about 0.5 K smaller (being below 1 K). This suggests, that some cloud contamination, potentially also sub–pixel scale, is present in the total IR CSR product. This has been considerably reduced due to the processing change at CIMSS, but is probably not fully eliminated. As noted in Köpken et al. (2002), the geostationary data show in their hourly data a diurnal cycle in the departures over sea. This is attributed to the observation of real changes in sea skin temperatures that are not modelled in the first guess.

2.2 Clear–sky radiances from Meteosat–5 and Meteosat–7

The Meteosat WV and IR CSR keep being monitored continuously within the operational system. The WV channel of Meteosat–7 is being assimilated (since 9 April 2002), while the active usage of Meteosat–5 is postponed until issues linked to the variation of the satellite's position are resolved.

2.2.1 Update on monitoring diagnostics

The monitoring versus the model first guess shows currently a mean departure of about 3.3 K and 2.5 K for the WV channel of Meteosat–7 and Meteosat–5, respectively. As discussed in Köpken et al., 2002, about 0.7 K of this bias is contributed by RTTOV–6M, so that the current bias estimate is about 2.7 K and 2 K for Meteosat–7 and Meteosat–5, respectively. These departures have been very stable over the last year. If the mean biases diagnosed for Meteosat–5 are influenced by the effects described Section 2.2.2 (e.g. through the cross–calibration) needs to be verified based on a longer data set, but no big changes are expected.

The IR channel currently has a bias of about -3.5 K for Meteosat–7 (-4 K for Meteosat–5) for all CSR data, and -3 K (-3.5 K) if only the CSR with a 100% clear sky fraction are considered. This is a stronger negative bias than reported for spring 2002, the negative bias having grown during the second half of 2002. The reason for this is not clear, but further investigation of the biases in the IR channel are clearly desirable.

Comparisons with other relevant satellites are done continuously as part of the monitoring and conclusions are basically unchanged since Köpken et al. (2002). Independent direct cross–calibrations between Meteosat and NOAA satellites (using HIRS–12 and AVHRR channel 3) have since confirmed these results (done at CIMSS, personal communication). This furthermore supports the approach followed here, that the comparison of different instruments versus the model first guess (in terms of TBs) can serve as an indirect cross–calibration between satellites.

As a complement to the disk means shown in Figure 9 and Figure 10 in Köpken et al. (2002), Figure 6 displays results within the common overlap area of Meteosat–7 and GOES–8 for the WV and the IR channels for a time period when both satellites are actively used in the assimilation. The GOES–8 data agree in the mean to within 0.5 K with the model first guess (for IR only if 100% clear CSR are considered). Meteosat–7 is about 2.5–3 K warmer in the WV (taking the 0.7K RTTOV bias into account) and about 2–2.5 K colder in the IR. The standard deviations of departures are almost identical in the WV (1.5–2 K). In the IR channel, the Meteosat–7 CSR show systematically higher standard deviations during daytime (up to 2 K), an effect which is less systematic, but still

present for the 100% clear data. This probably points to less cloud contamination in the GOES CSR, which may be explained by a better cloud detection being possible due to the presence of the additional IR channels, esp. the 3.9 μm. With MSG even more improvements in that respect are expected. Based on this cross–comparison and the previous results, it is still believed that the Meteosat satellites display a positive bias in the WV and a cold bias in the IR.

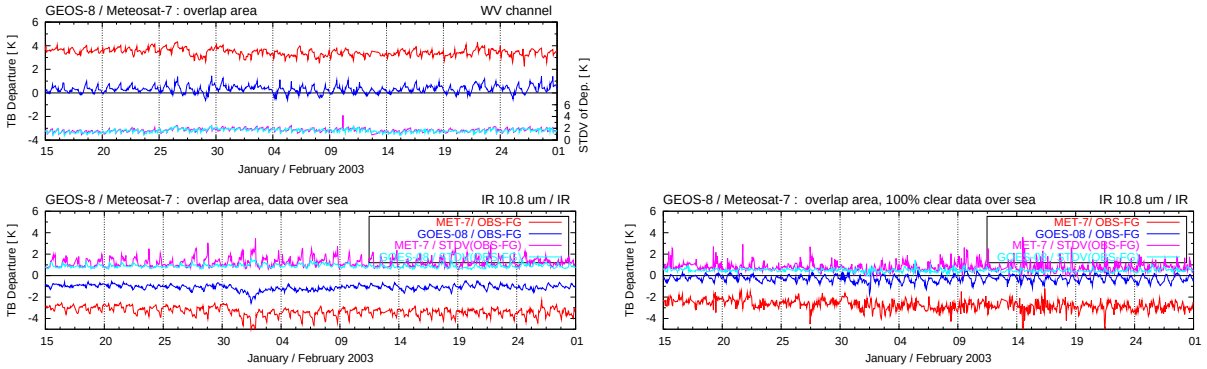

Figure 6: Top: Time series of mean differences between TB (K) of observations and model first guess for the WV channels of Meteosat–7 (red curve) and GOES–8 (blue curve) for data within a common overlap area (-55°to -30°Lon, 30°to -20°Lat) for 15 January to 1 March 2003. Standard deviations of departures are also shown (pink for Meteosat–7, light blue for GOES–8). Bottom: as top, but for GOES 10.7 μm and Meteosat IR channel and for all data over sea (left) and the subset of data having a 100% clear fraction (right).

2.2.2 Influence of variations in orbit position of Meteosat–5 on CSR

Figure 7 illustrates an effect which showed up in the Meteosat–5 data as an oscillation in observation minus first guess departures. These oscillations are only visible when looking at statistics for separate latitude bands and have an amplitude of 1K with opposite signs in the northern and the southern latitude stripes (second and fourth panel). Over the whole disk, the effect therefore vanishes. The times of the minima and maxima change throughout the year (curves for January and June shown here) and coincide with spikes caused by solar stray light during spring and autumn (compare January in southern hemisphere). This suggested a link to the satellite's orbit. The geographical representation in Figure 8 shows that the effect is indeed a homogeneous positive and negative bias anomaly in both hemispheres. The observed bias patterns could quickly be linked to the inclination of the satellite around it's nominal position of 0°latitude (Leo van de Berg, personal communication).

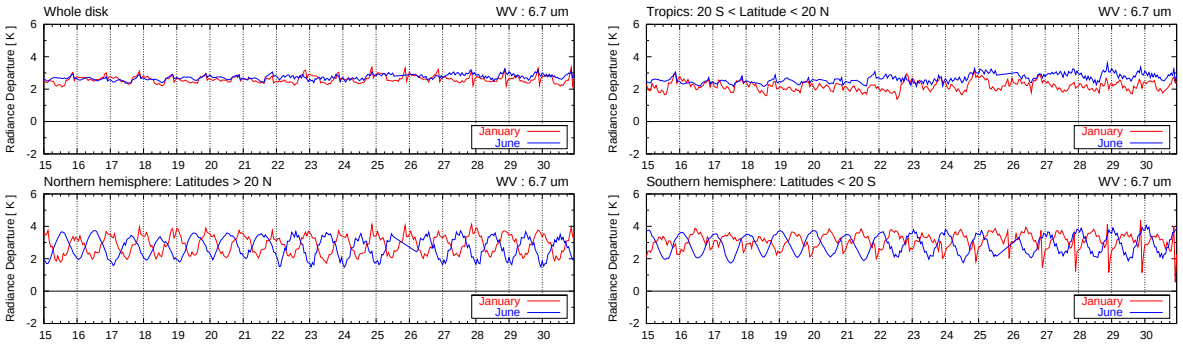

Figure 7: Time series of mean differences between WV CSR observations and model FG TB for the whole disk, and the three latitude bands >= 20 °N, ±20°N/S, and <= 20°S for days in January (red curves) and June (blue curves).

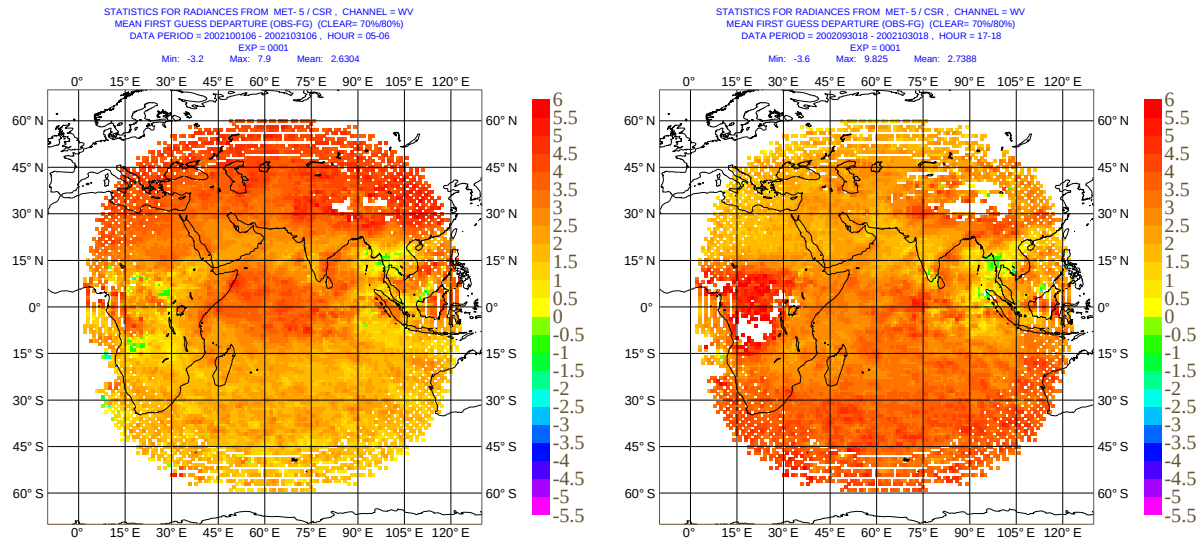

Figure 8: Mean TB difference between WV CSR and first guess for data at 6 UTC (left) and 18 UTC (right) during the month of October 2002.

While for Meteosat–7 the inclination is controlled to stay within $\pm 1°$, the inclination is no longer controlled for Meteosat–5 in order to save fuel. The satellite therefore travels on a daily figure of eight pattern up to 5°inclination away from the equator.

The processing at the Meteorological Product Extraction Facility has now been changed and the varying satellite inclination is taken into account, influencing particularly the satellite zenith angle for the observations. 15 hours worth of data from the updated system have been transferred and tested at ECMWF and the effect seems to be properly removed. Figure 9 shows on the left the difference in zenith angles between the updated and the currently operational CSR data. It reaches up to $\pm 6.5°$. This causes differences in the calculated first guess TB of up to 1 K. The most noticeable change in the CSR observations themselves is a drop in the number of CSR data by about 14% and 17% in the IR and WV channel, respectively (the cloud detection at the MPEF uses radiative transfer calculations based on the ECMWF first guess and will therefore be influenced by the currently incorrect zenith angles). There is hardly any change, though, in the values of the CSR where data are derived both in the test and the operational system as seen in the bottom panel for WV. Results for the IR CSR are similar. Nor can any systematic change be seen in the corresponding first guess departures. A small improvement in the IR over sea at extreme latitudes will need confirmation based on a larger data sample. The bottom panel shows time series of first guess departures for the test data in comparison to the operational data. As expected, the oscillation is gone and it is anticipated that after transfer of this patch the Meteosat–5 radiances prove stable so that an assimilation may be envisaged. The impact of the oscillations on the cross–calibration procedure are currently under investigation at EUMETSAT.

2.3 Preparations for MSG and additional GOES satellites

In order to prepare for the contribution of ECMWF to the calibration and validation phase of MSG, the ECMWF system has been prepared to allow the processing and monitoring of MSG radiances. Apart from necessary modifications in IFS, a pre-thinning and screening program has been set up to allow adjusting the increasing data volume passed through the system in a flexible way. The preparations also included specifically the development of the new monitoring package 'satmon' (in cooperation with two other consultants) which has been designed to allow a more comprehensive and flexible monitoring for different satellite systems, including MSG, in one framework. This will allow an extensive feedback on MSG radiances to EUMETSAT and has

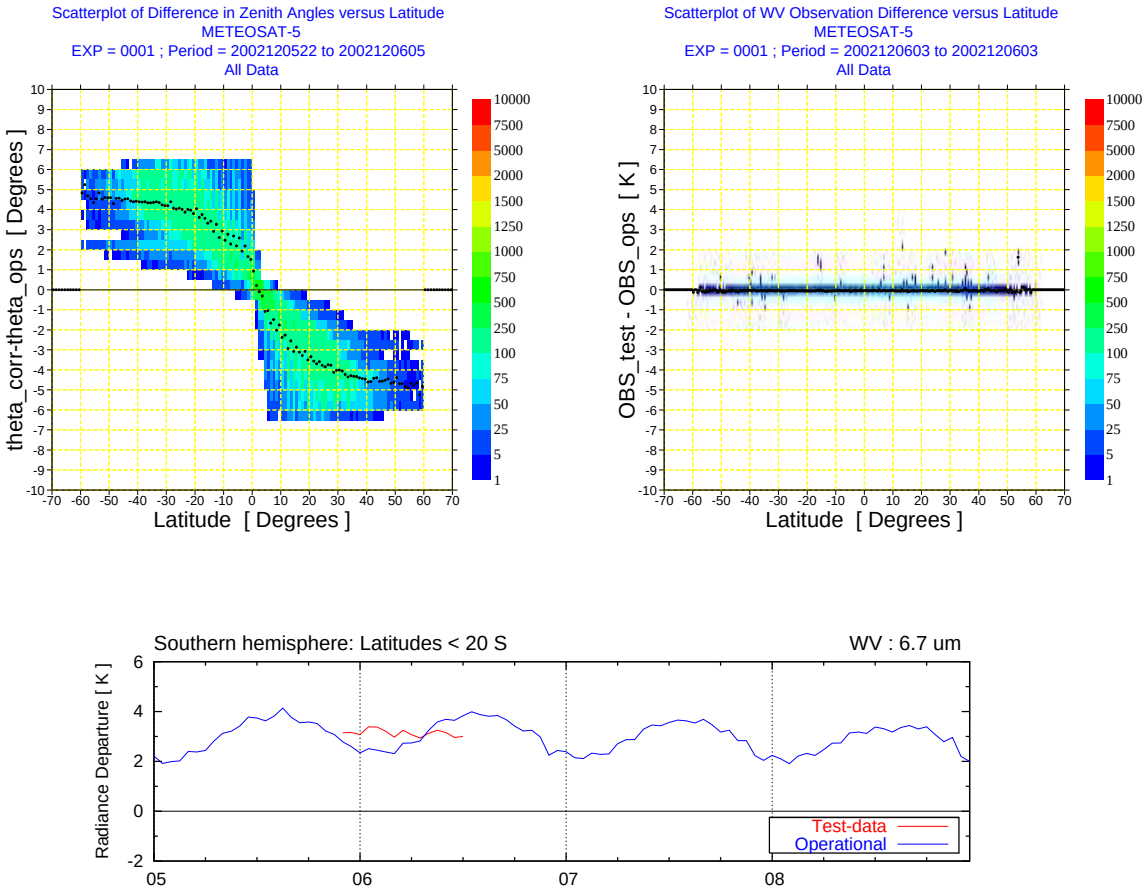

Figure 9: Left: Scatter plot of differences in CSR zenith angle between the test and the operational data versus latitude (for data between 22 UTC 5 December and 5 UTC 6 December). Right: Scatterplot for the difference in CSR in the IR window channel between the test and the operational data versus latitude (for data at 3 UTC, 6 December). The colour scale gives the number of data in each bin, the black dotted line indicates the mean within each latitude bin. Bottom: Mean WV CSR observation minus first guess departures for the operational data (blue) and the test data (red) for 5 to 7 December 2002. Test data were obtained from 22 UTC 5 December until 12 UTC 6 December.

already proven useful in the monitoring of the current Meteosat and GOES data. A web-interface to the plots has been set up (main work done by Pauline Butterworth) which allows online display of statistics versus the ECMWF model as well as of comparisons to other satellites (indirect 'cross–calibration'), see Figure 27 in the appendix for an example webpage layout. The end–to–end testing and finalization of the setup for MSG is pending availability of test data.

Additionally, the IFS has been prepared to accomodate GOES–9 and GOES–12 imager data which will become available early in 2003 for the Pacific (GOES–9 replacing the Japanese GMS) and for the Americas (GOES–12 replacing the currently operational GOES–8).

An effort of homogenisation of the BUFR data formats used by CIMSS and EUMETSAT has been undertaken and new common BUFR templates have been approved in 2002 by WMO for radiances from imagers with either three or up to 12 channels. This new format is now used by EUMETSAT since 2 December 2002 (BUFR descriptor 30024, 3 channel data) and by CIMSS (BUFR descriptor 310023, up to 12 channel data) since end of January 2003 in parallel to the current format. In the near future, the MSG CSR data will also be encoded using BUFR descriptor 310023, so that only one format then needs to be dealt with, easing technical maintenance issues. However, the quality information supplied by the different satellite data producers along with the CSR data varies.

3 Assimilation of GOES WV radiances

3.1 Data selection

In addition to the first guess checks and the variational quality control checks Andersson and Järvinen (1999), further quality checks are suggested by the GOES monitoring results (see Section 2.1.2). For dealing with the change of biases around local midnight there are two basic approaches. One is to exclude the data while waiting for a correction of this anomaly by the satellite agencies. The other is to try correcting for the effect at the user's end, which could be achieved through a time dependent bias correction. This approach is being followed by the NCEP (XiuJuan Su, John Derber, personal communication) and also by CMC (Louis Garand, personal communication) where the use of 6 hourly data in a 3DVAR asimilation is investigated. The approach then can be to derive two different sets of bias correction coefficients, one for the data slot closest to local midnight (6 UTC for GOES–8 and 6 and/or 12 UTC for GOES–10) and one for the other times of day. In a 4DVAR context, using all the hourly data over a 12h time window, however, this concept becomes more difficult to realize, as a smooth transition between the different biases takes place (see Figure 3). Therefore, the first approach is chosen here. Based on the monitoring results and on the theoretical evidence (Johnson and Weinreb, 1996), the excluded images/data currently are 2–8 UTC for GOES–8, and 7–10 UTC for GOES–10. As for Meteosat, CSR having satellite zenith angles larger than 60° or being over high terrain (higher than 1500 m model orography) are also excluded.

Further quality control aims at excluding data with potential cloud contamination. In histograms of the WV and the IR channel departures a characteristic 'cold tail' can be seen. As for the Meteosat CSR, a small dependence of the departures on the clear–sky fraction in the CSR can be found. The left panel in Figure 10 shows this for GOES–10 data. An additional check is the scatterplot in the right panel showing first guess departures of the WV CSR versus those of the IR CSR for data over sea, here for GOES–8 (results for GOES–10 are similar). It can be seen that the distribution is not symmetric around the axis of the mean WV bias (1.6 K). The distribution is particularly skewed for very negative departures in the IR, which points to cloud contamination also in the WV channel. Therefore, data points over sea having IR departures more than 3 K colder that the mean IR bias are excluded. The IR departures over land not being as reliable due to a bigger uncertainty in the skin temperature and emissivity, the criterion over land is based on the clear–sky fraction. A threshold of at least 40% clear pixels within the CSR was chosen based on various scatterplots or different periods. Independent

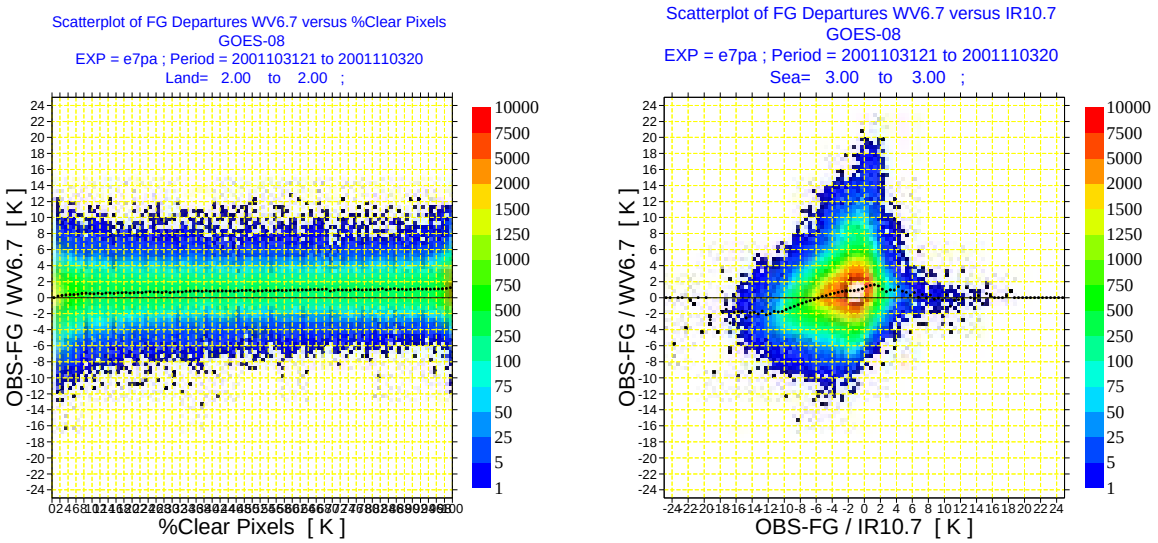

Figure 10: Left: Scatter plots of observed WV CSR minus model first guess (as TB in K) versus the clear–sky fraction within the CSR segment for data over land from GOES–8 for the period 31 October to 3 November 2001. Right: as left, but versus the first guess departures of the IR channel for data over sea.

diagnostics at NCEP resulted in choice of the same threshold (Su, personal communication).

During the thinning of satellite data done within the assimilation step, CSR data having the highest fraction of clear–sky pixels and high associated infrared TBs are chosen. It is noted, however, that such a selection may have a tendency to bias the analysis to drier conditions (note that this is true in general also for the current usage of clear–sky radiance information only from both polar orbiters and geostationary satellites). However, during the experiments no overall systematic drying is found and results seem to slightly improve the fit to radiosonde information and a positive forecast impact is obtained (see Sections 3.2.1, 3.2.2). Therefore the current approach is followed with the aim to select the data least likely to be cloud affected. Revisiting these selection criteria, e.g. based on independent cloud information from more comprehensive radiometers like MODIS, may allow improving the data selection.

3.2 Assimilation experiments

Assimilation experiments have been conducted using the WV CSR from both GOES–10 and GOES–8. In the following, results will be shown from two assimilation experiments using all operational observations including Meteosat–7 WV CSR, HIRS–12 radiances from NOAA–14, and geostationary AMVs. It should be noted, that for the GOES satellites the AMVs are currently assimilated based on the 'SATOB format' in which no distinction is being made between the WV winds originating from cloudy and clear–sky areas. Therefore, the control experiments not using the GOES CSR will also contain information on the wind field in clear–sky as provided through the AMVs. Although this information is not assimilated in an optimal way, as the height assignment of these winds does not take the thick layer from which the clear–sky radiation emanates into account, one may expect that this can reduce the impact achieved through the GOES WV CSR data which also contain wind information through their time sequence. Also, this means that related observational information is used in two different forms at the same time which is clearly not optimal. However, the CSR provide at least additional upper tropospheric humidity information. Once the GOES AMVs can be used in the 'BUFR format' distinguishing between the types of winds, an additional experiment excluding the clear–sky WV winds should be performed.

Of the experiments shown, one was like operations at T511 resolution and 12 hour 4DVAR for the period 20 February to 20 March 2002 and in parallel to the pre–operational system including the Meteosat–7 assimilation (experiment named e97n). Another experiment was conducted at lower resolution (T319, 6 hour 4DVAR) for the period 1 February to 4 March 2002 and had a stricter quality control by excluding the slots affected by the midnight problem described in Section 2.1.2 (experiment named e9au). The choice of the slightly different period for the lower resolution experiment was determined by the availability of a control experiment (reasons of computation time).

Figure 11 shows in the top panel the mean change in upper tropospheric humidity (here relative humidity at 300 hPa) due to the assimilation of WV CSR from GOES. Within the area covered by GOES–8 and –10 there is characteristically a decrease of upper level humidity in the convective areas of the Inner Tropical Convergence Zone (ITCZ) and the Southern Pacifi c Convergence Zone (SPCZ) while humidity is increased in adjacent areas (changes being about 2-10 %).
The scattered humidity changes outside the GOES areas are caused by a slightly different evolution of weather

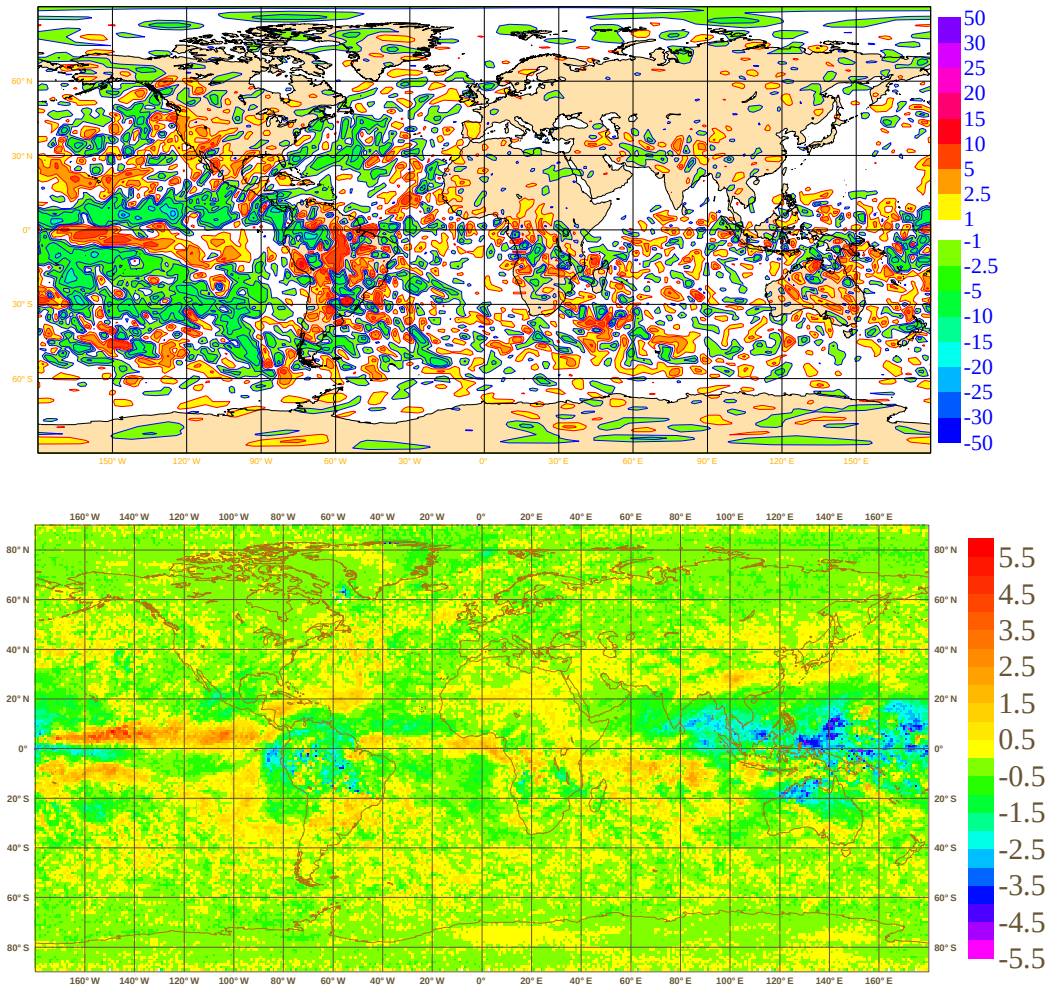

Figure 11: Top: Mean difference in analyzed relative humidity (in %) at 300 hPa between the experiment assimilating GOES WV CSR and the control. Average is from 1 February to 3 March 2002 for 00 UTC analyses. Bottom: Mean difference of HIRS channel 12 (NOAA-15, bias corrected) minus FG as brightness temperature (in K) averaged onto a 1° grid over the period 1 to 28 February 2002.

patterns between the assimilation experiment and the control. The systematic humidity changes in and around the ITCZ are also found over the Atlantic in assimilation experiments with Meteosat–7 CSR (Köpken et al., 2002). This influence of the WV radiances is consistent with the model being known to have a too static and hence too moist ITCZ. The increments caused by the geostationary WV CSR are also consistent with other radiances, as illustrated in the bottom panel: The HIRS–12 observations show also higher TB than the model in the ITCZ and SPCZ, corresponding to a drier (and possibly warmer) upper troposphere as compared to the modeled conditions. This correspondence with the HIRS observations leads to an improved fit of the model first guess (and analysis) to HIRS observations when the GEOS WV CSR are assimilated.

3.2.1 Verification versus observations

As found for the assimilation of Meteosat–7 CSR, the fit to conventional observations remains mostly unchanged. For some variables and areas, small improvements can be seen. Figure 12 shows the fit to radiosonde humidity observations for the southern hemisphere areas covering the GOES–8 and GOES–10 disks. The model displays in both areas a positive humidity bias with respect to the radiosondes, especially above 300 hPa. The radiosonde information is only assimilated up to this level. This positive bias is slightly reduced when GOES data are assimilated. Radiosonde observations of humidity have to be taken with care, particularly at high levels (low temperatures). Still, it is interesting to note that the GOES data support the radiosonde data at least in tendency. Also, the root mean square error (rms) of the first guess with respect to the radiosondes is

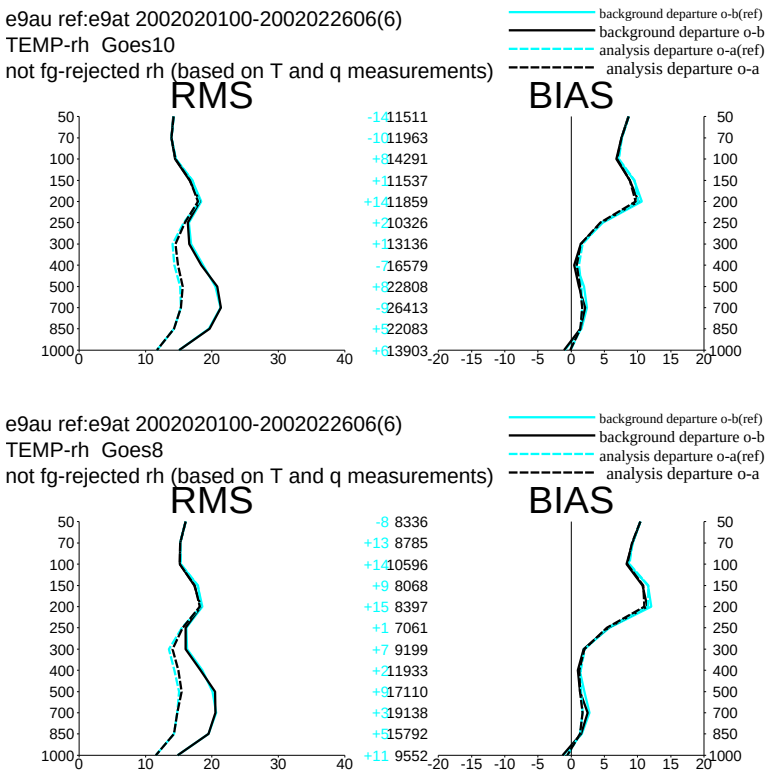

Figure 12: Statistics of departures between relative humidity observations from radiosondes (for data not rejected in FG check) and model FG (solid lines) and analysis (dashed) for the experiment with assimilation of GOES WV CSR (black lines) and control (blue). Root mean square errors are on the left, biases (observations minus model) on the right; the number of data are given in the middle (blue numbers give differences in data usage, '+' signifying more data used when assimilating GOES data); period is 1 February to 26 February 2002. Top: results within square covering GOES–10 disk, bottom: for GOES–8 area.

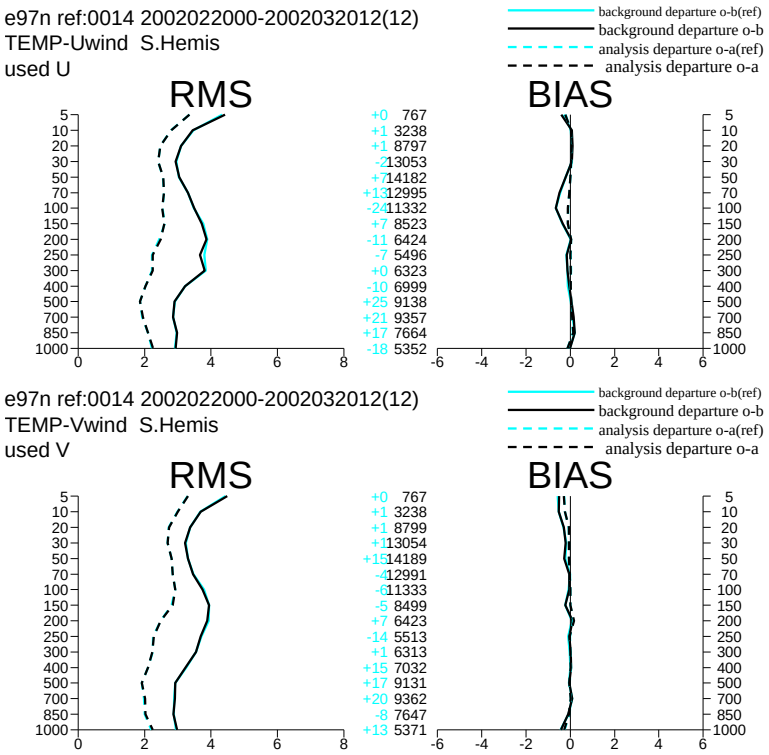

Figure 13: Statistics for departures between used wind observations from radiosondes and model FG and analysis for the period 20 February to 20 March 2002 (plot layout as in Figure 12). Top for U–component, bottom for V–component of the wind vector.

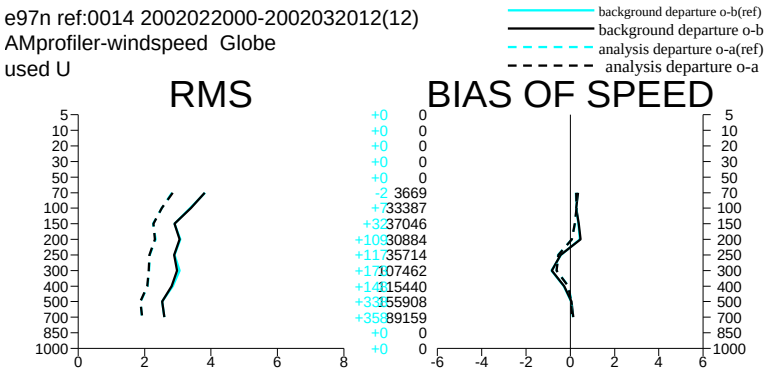

Figure 14: As Figure 13, but for comparisons to used American wind profiler observations (in terms of wind-speed, m/s).

slightly reduced when GOES CSR are used which is a good sign. For the analysis there is also a small reduction of the bias around the levels 150 and 200 hPa. The rms is slightly larger in case of the assimilation of GOES WV radiances as may occur if additional data are introduced. The results for GOES–8 and GOES–10 areas look very similar. In the tropical and northern hemisphere parts of the GOES disks, the fit of the model to the observations is unchanged.

In terms of influence on the wind fields, Figure 13 shows a small, but distinct improvement in the agreement of the first guess wind at 250 hPa with radiosondes for the southern hemisphere observations, while the statistics for other latitude bands are unchanged. A similar positive signal is found for wind observations from aircraft (not shown). With respect to observations on the northern hemisphere, a small degradation for the fit of the v–component of the first guess to observations of the European windprofiler network is seen, which is unexplained.

It is very encouraging, though, that for wind observations from the American wind profiler network, there is a slightly improved rms fit for both the u– and v–components of the wind vector, mostly around the 300 hPa level. Figure 14 illustrates this, showing the statistics in terms of windspeed. Also, there is a tendency for more wind profiler observations to be assimilated (although it is only a small change compared to the overall amount of observations used).

3.2.2 Impact on forecast quality

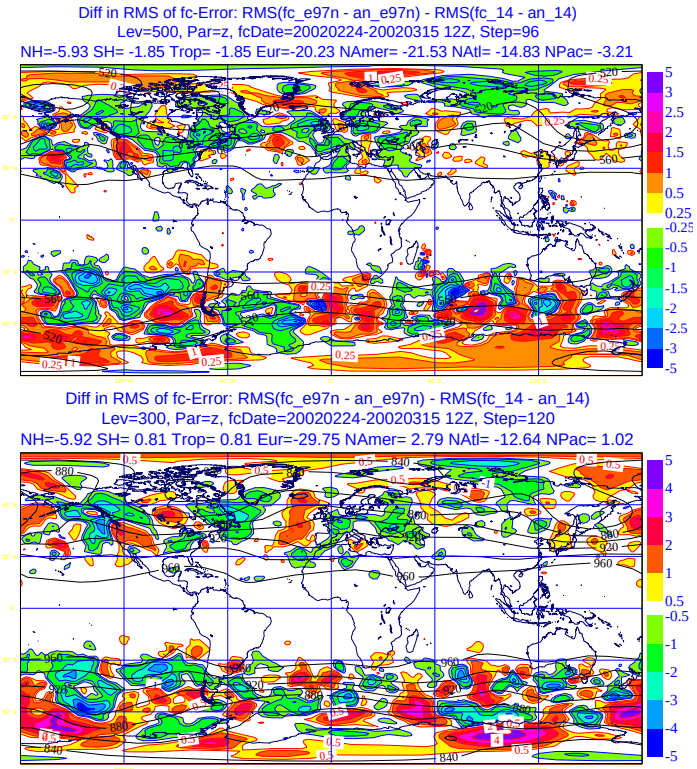

Figure 15: Difference in forecast errors (root mean square of forecast minus verifying analyses) between the GOES WV assimilation experiment (named e97n) and its control for forecasts from 24 February to 15 March 2002. Top: for 4 day forecast of 500 hPa geopotential; bottom: for 5 day forecast of 300 hPa geopotential.

Figure 15 shows the geographical distribution of forecast errors for the 12h 4DVAR experiment. Green areas, indicating smaller 4 day forecast errors for the 500 hPa geopotential when GOES CSR are assimilated. They dominate especially on the northern hemisphere. It is particularly visible for large areas over northern America and parts of the Atlantic, both downstream of the areas covered by the GEOS satellites. On the southern hemisphere the picture is more mixed, but positive impact can also be seen on the west of the southern Atlantic. The overall impact is still slightly positive. For higher levels the bottom plot shows the impact for the day 5 forecast, this time positive influence of the data being found over the west north Atlantic, over areas of the northern and southern Pacific and also further downstream.

Results in terms of anomaly correlation (top panels) and root mean square errors of the forecasts with respect to the verifying analyses are shown in Figure 16 (here for the experiment excluding data around local midnight). There is a small but statistically significant positive impact on the southern hemisphere while for the northern hemisphere as a whole this experiment was neutral. Larger positive impact is found over the northern Pacific and northern America.

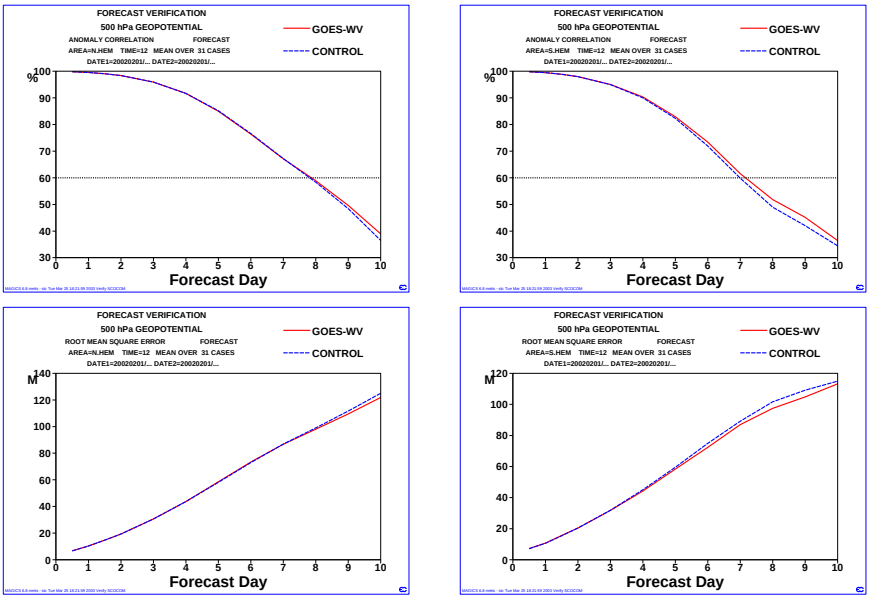

Figure 16: Anomaly correlation and root mean square error of 500 hPa geopotential for forecasts up to 10 days verified against operational analyses for the experiment with assimilation of GOES–8 and –10 WV CSR (solid line) versus the control (dashed line). Left panel is for the Northern hemisphere (> 20°N), right panel for the Southern hemisphere (< -20 °S). The average comprises 31 cases from 1 February to 3 March 2002.

4 Structure of humidity increments and use of revised humidity formulation

The structure of increments is determined by the observation innovation, i.e. the difference of observation minus first guess at the observation locations, and by the correlations of the model's background errors (Derber and Bouttier, 1999), the amplitude being driven by the ratio between observational and background variances. Figure 17 shows an example of relative humidity increments for a 3DVAR analysis in which only observations are Meteosat–7 WV CSR. In this 3DVAR analysis, increments are confined to the area of the Meteosat observations, any increments outside being explained in terms of the horizontal correlations in the background errors. Due to the high density of the geostationary radiances, the horizontal structures of the increments reflect primarily the observation innovations and less the broader scales of the background errors. It is interesting to note that in the case of 4DVAR, more increments (in both humidity and wind fields) occur also outside the disk covered by the data and especially on the upwind side.

An example of the vertical stucture of increments is illustrated in Figure 18 which displays a cross section through analysis increments from a 3DVAR experiment in which only Meteosat–7 data were assimilated. The increments typically occur between 100 and 700 hPa, peaking at 300 to 400 hPa. The peak and vertical extent of the increments clearly reflect the Meteosat WV channel sensitivity (weighting function). Increments from HIRS–12 data have similar vertical structures, while HIRS–11 data induce increments also lower in the atmosphere. The vertical influence due to the channel's weighting function is modulated by the background errors and their vertical correlation functions (based on forecast error statistics) which increases the vertical extent and shifts the peak of the increments slightly downwards. As can be seen at e.g. 39°N in the cross section, increments may even extend down to the surface despite the fact that the WV channel is not sensitive to the low levels of the atmosphere. Such increments arise from correlations in the background errors between higher and low levels. If there are no other observations sensitive to humidity at low levels, no observational constraint is present to prevent such analysis increments. This is the case in this 3DVAR using only Meteosat–7

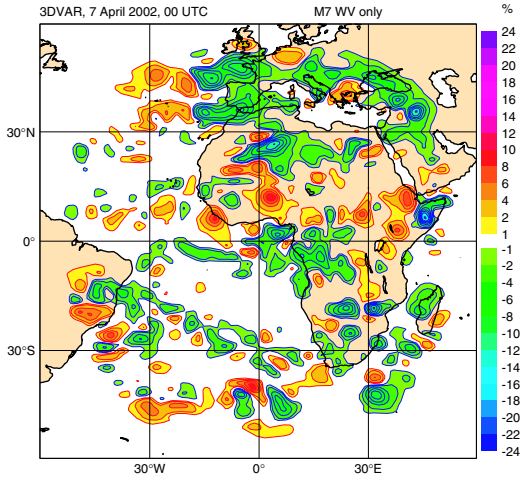

Figure 17: Relative humidity increments (analysis minus first guess, in %) at 400 hPa for a single cycle the 3DVAR analysis for 7th April 2002, 00UTC using only Meteosat–7 WV CSR.

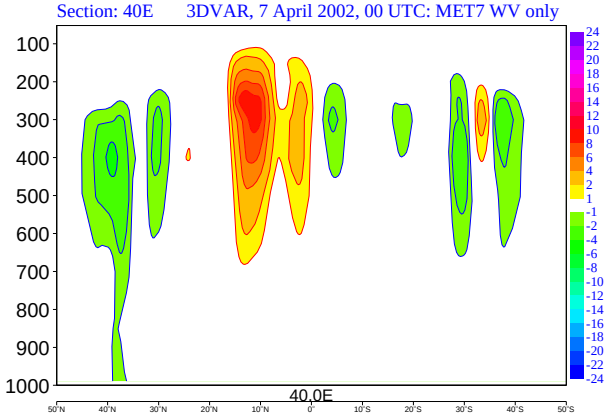

Figure 18: Vertical cross-section (versus pressure in hPa) of the relative humidity increments (analysis minus first guess, in %) at 40°E for the 3DVAR FGAT experiment for 7th April 2002, 00 UTC.

CSR, but will also frequently happen in real analysis situations. It is likely that physical parameterizations, e.g. convection, are sensitive to these increments.

For the humidity analysis variable, a new formulation has been developed (Holm 2002 and Holm et al., 2002) which is based on a scaled relative humidity instead of the specific humidity that is used currently (described in Rabier et al., 1998). The advantage of this revised formulation is that background errors have a much more gaussian distribution (when characterized for each vertical level) than is the case for specific humidity. Therefore, the basic assumption of gaussian error distributions for model errors is better fulfilled. Along with the background error variances, also the background error correlation structures for the humidity variable are changed. Therefore, the weights that observations receive under certain conditions will change as will e.g. the vertical spreading of increments. Figure 19 shows an example of background errors in terms of brightness temperatures for HIRS channel 12 (and Meteosat WV channel) which are computed using the randomization procedure described in Andersson et al. (2000). In the currently operational analysis system (top panel), the background errors (σ_b) show very marked variations over the globe, exceeding 5 K in many areas, particularly under dry sub–tropical atmospheric conditions. This is illustrated further in Figure 20 (left panel), which shows background errors reaching 5–15 K under very warm and dry conditions (high observed TB values). This

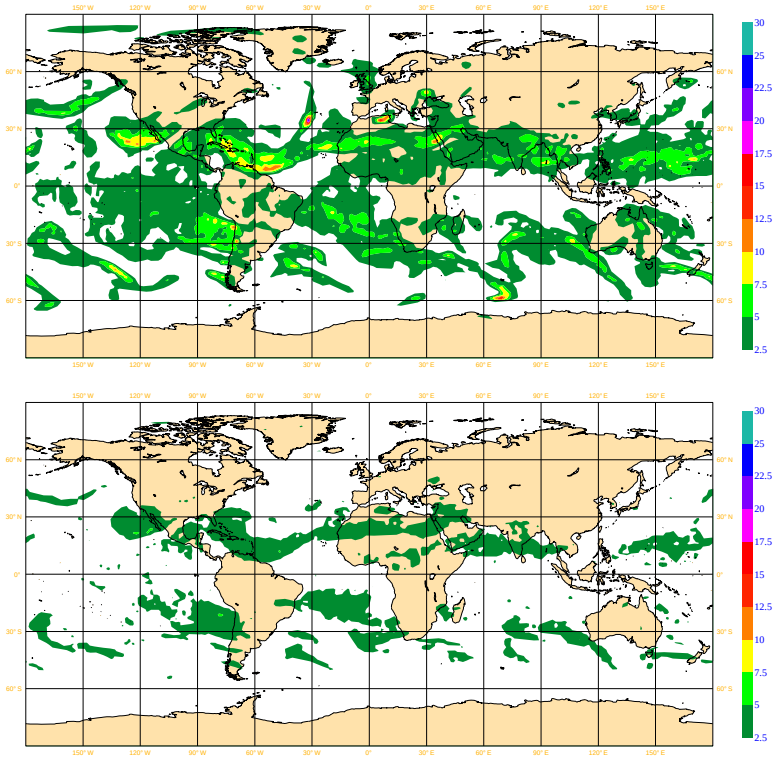

Figure 19: Example of background error standard deviations for Meteosat WV channel in terms of brightness temperatures (in K; similar to those for HIRS channel 12) for the analysis of 25 Janurary 2002, 00 UTC; shading only for errors larger than 2.5 K. Top: for the currently operational humidity analysis variable (specifi c humidity). Bottom: for the new variable (scaled relative humidity).

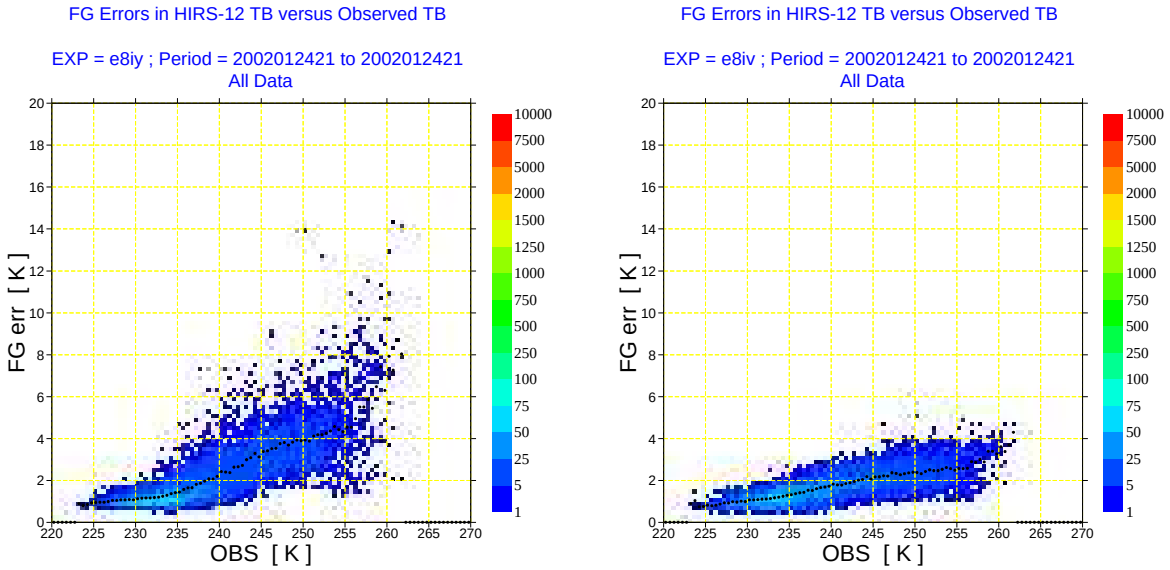

Figure 20: Background error standard deviations for Meteosat WV channel (and HIRS channel 12) as in Figure 19, but as scatterplot versus the TB observations. Example for the date 24 January 2002, 18 UTC for the operational (left) and the new (right) humidity analysis formulation.

leeds to excessive weight given to the 6–micron humidity–sensitive channels like HIRS–12 and the Meteosat or GOES WV channels. Andersson et al. (2000) investigated this problem in the context of poor convergence of the minimization, which led to a fi x introducing an empirical upper limit for humidity errors. The still locally occuring large ratios between σ_b and σ_o (the observation errors are set to 2 K for the WV channels) result in poor conditioning of the minimisation problem and a slow rate of convergence. The large values are also in contradiction with the statistics of observation minus fi rst guess departures which have an rms of 2.5–5 K in dry sub–tropical regions. For the new humdity analysis, these extremely high σ_b are avoided. Figure 19 (bottom) and Figure 20 (right) show that for the new humidity analysis variable σ_b nearly always stays below 4 K. Also, in dry sub–tropical air (high observed TB), the mean of σ_b is close to 2.5 K which is in good agreement with departure statistics, thus indicating that these data will get approximately the correct weight in the new humidity analysis.

In accordance with these changes in the background errors, the amplitude of increments is found to be diminished in many areas, especially in cases of very large analysis incrments, while the patterns (determined by the observations themselves) remain unchanged (Figure 21). Figure 22 illustrates this further by showing increments for two profi les occuring in areas of big increments in the current analysis. The profi les show humidity increments for the current formulation (blue) and for the re–formulated (magenta) humidity analysis, respectively. The humidity increments are generally smaller with the new formulation. It should be noted that there is also less extrapolation of humidity increments to the lower troposphere due to reduced vertical background error correlations between the upper and lower levels (see example in left panel). Often, the increment profi les tend not to be smooth but to display spikes, both in the current and the new formulations. This is caused by the σ_b depending on the value of the background humidity itself. E.g. the σ_b of specifi c humidity in the current formulation is small in dry conditions, so that the analysis increments at that level are strongly constrained. Also with the new formulation, the σ_b of relative humidity is smaller close to saturation or for very dry conditions (avoiding analysis increments causing unphysical relative humidities). In the fi nal implementation, the scheme will be used in a non–linear version, in which the increments are added in the outer loops (between the actual minimization loops done at lower resolution) with an additional factor depending on background relative hu-

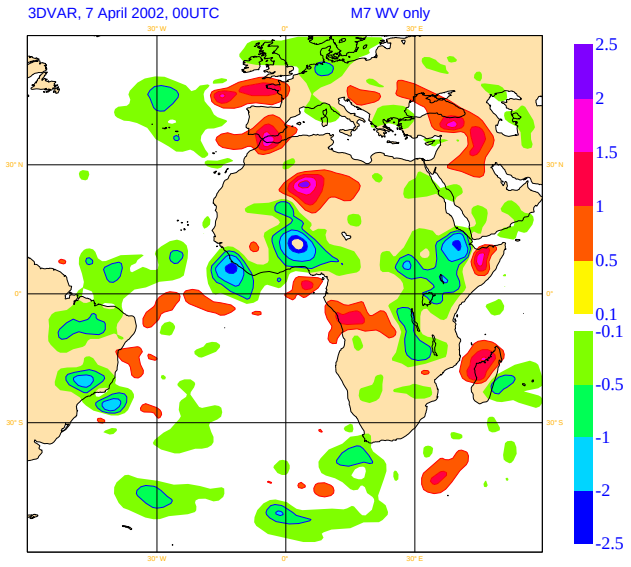

Figure 21: Difference in relative humidity increments (in %) at 400 hPa between analyses using the current and the new humidity variable formulation; for the same single cycle 3DVAR analysis for 7th April 2002, 00UTC using only Meteosat–7 WV CSR as in Figure 17.

midity allowing assymetric larger increments in areas close to saturation and at very dry conditions. This factor assures that observations indicating much drier conditions when the first guess is very close to saturation to cause larger negative increments (and vice versa). Experimentation with this enhanced formulation is ongoing.

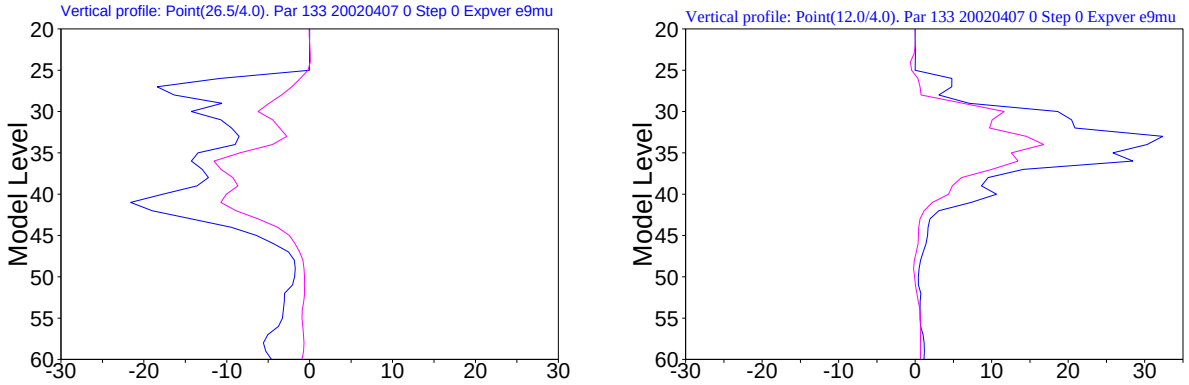

Figure 22: Two selected vertical profiles of humidity increments at a location with negative (left) and positive (right) increment from the 3DVAR analysis shown in Figure 17 (00 UTC 7 April 2002, using Meteosat–7 CSR only). The increments are expressed in percent of the background value of q for the operational (blue) and the new (magenta) formulation of the humidity analysis.

5 Reprocessed geostationary CSR in the ERA–reanalysis

The ERA–40 reanalysis creates a state–of–the–art dataset of atmospheric analyses covering the period mid–1957 to 2001 using a 3–dimensinal variational analysis with 6 hourly cycling and at a resolution of approx. 125 km (for further documentation, see ERA–40, 2001). In support of this project, EUMETSAT has reprocessed Meteosat–2 data for the period 1983–1988 with the current processing algorithms. Together with the atmospheric motion winds, which are of better quality compared to the old operational product, also the CSR have been produced which had not been available at the time. The model setup used for ERA and the current model versions have been adapted so that data from the early satellites Meteosat–1 to Meteosat–4 can be processed (i.e. particularly regression coefficients for transmittances and surface emissivities have been derived for RTTOV–5 to RTTOV–7, courtesy P. Brunel, R. Saunders). Available Meteosat–2 CSR have been passively monitored to assess their quality with a view to their possible assimilation in future reanalysis projects.

Meteosat–2 data are expected to be noisier than for Meteosat–7, since the data are encoded with less accuracy (Meteosat–7 uses 8-bit for all channels, while for Meteosat–2 uses only 5 bit for the WV channel and 6 bit for the VIS channel). The higher noise level is clearly visible in the WV imagery. Also, the cloud detection, being a prerequisite for the CSR product, will be made more difficult by these technical limitations. The number of CSR data derived is about 7% higher for Meteosat–2 than for Meteosat–7 during a comparable period and 10-20% more CSR are in the category of at least 70% clear, so that higher residual cloud contamination is suspected for Meteosat–2. Several of the findings described below support this. Figure 23 shows scatterplots of the observation minus model first guess departures versus the standard deviation of the pixel TBs contributing to the CSR observations (based on a week of data from the initial test data set for July 1988 for Meteosat–2 and a week in July 2001 for Meteosat–7). It is clearly visible that the standard deviation of the pixels within the CSR is considerably higher for Meteosat–2 as compared to Meteosat–7, reflecting the higher noise in the original pixel data. However, the averaging implied in the creation of the CSR data diminishes this noise, so that the distribution of the first guess departures (and their standard deviation) is rather comparable for both satellites.

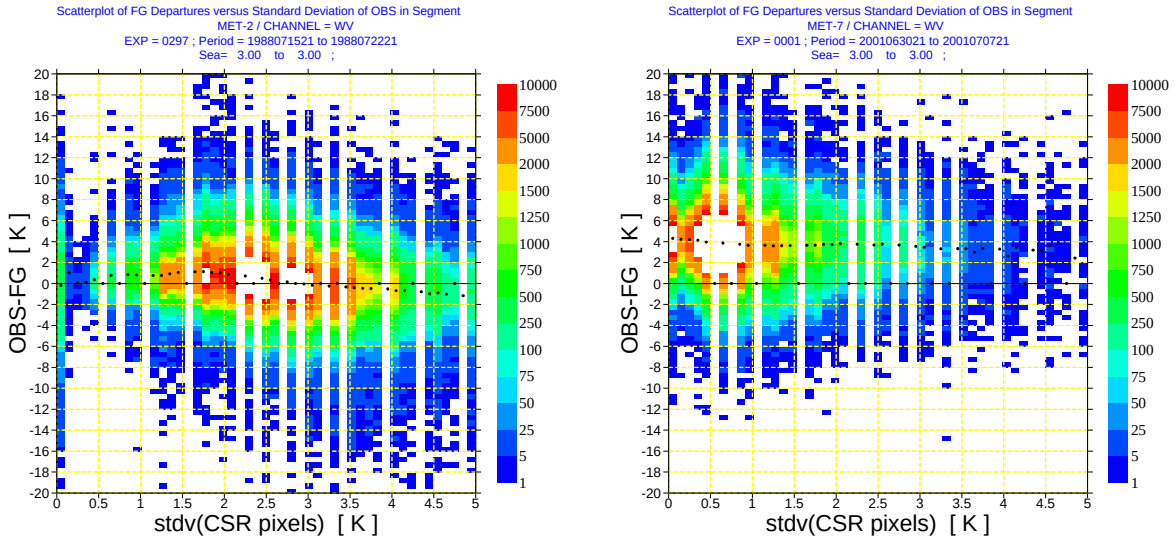

Figure 23: Scatter plots of observed WV CSR minus model first guess (as TB in K) versus the standard deviation of the TB of the clear pixels within the CSR segments (in K) for CSR data over sea. Left: for Meteosat–2 (data from the week 15 to 22 July 1988); right: for Meteosat–7 (data from week 1 to 7 July 2001).

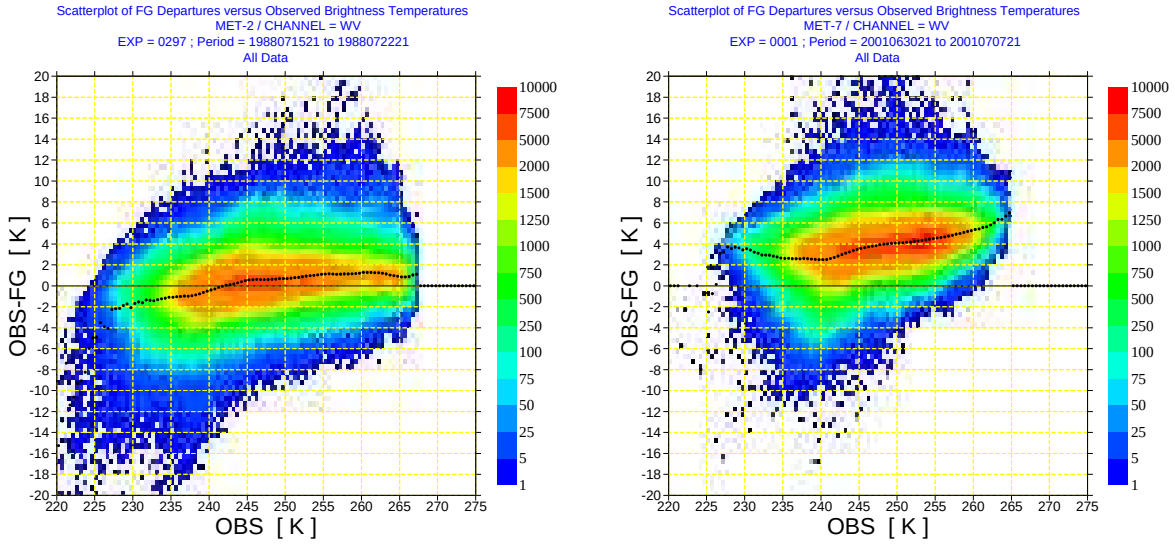

Figure 24: As Figure 23, but scatter plot of observed WV CSR minus model first guess (as TB in K) versus the observed CSR (as TB in K) for all data.

The dependence of the mean bias on percentage of clear pixels is also similar for both satellites, the bias over land varying by about 2 K between CSR data with low and high percentage of clear pixels (not shown). The distribution of first guess departures versus observed TB in Figure 24, though, shows that for Meteosat–2 there are more distinctly negative departures at low TB which is probably indicative of cloud affected CSR. This effect is much more pronounced over land than over sea, but also for data over sea this 'cold tail', indicative of cloud affected radiances, is stronger for Meteosat–2 than for Meteosat–7.

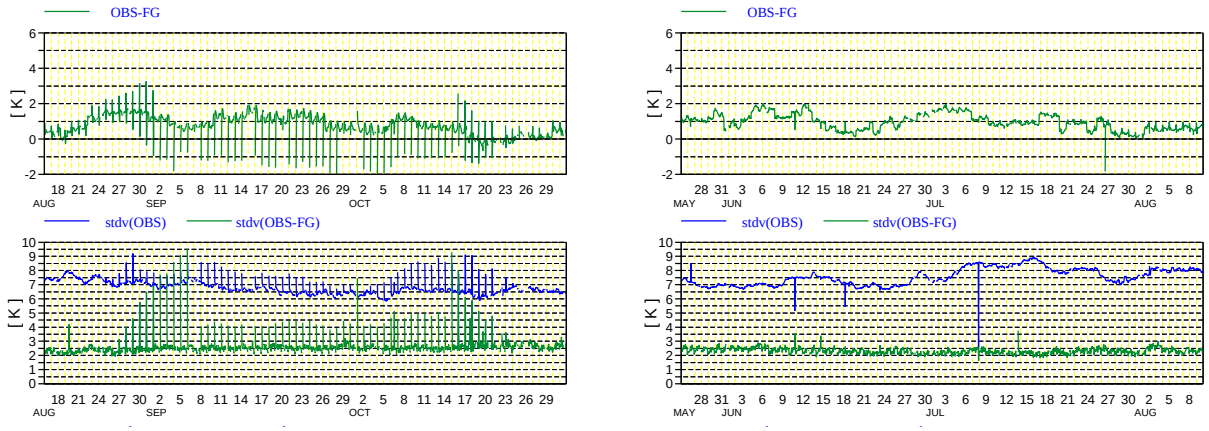

Figure 25: Time series of mean differences between WV CSR observations and model FG TB (top) and their standard deviations (bottom, green curve) and standard deviation of the CSR (blue curve) for the whole disk and Meteosat–2 data from 17 August to 31 October 1983 (left panels) and 27 May to 9 August 1988 (right panels).

Figure 25 shows examples of timeseries with the mean first guess departure and its standard deviation for August to October 1983 and June to August 1988. The mean bias is mostly around 1 K (dropping to nearly zero at the end of October 1983). This is different from the biases in the current Meteosat data which are about 3.5 K for Meteosat–7 and 2.8 K for Meteosat–5. Further investigation into why this difference between reprocessed Meteosat–2 data and current operational data occurs is necessary. The bias versus the model varies by about 1-2 K from day to day (or even within a day). This variation can be attributed to the use of the vicarious calibration as similar changes had occured for Meteosat–7 until the blackbody calibration was introduced (Köpken, 2001) and could be linked in time and magnitude to changes in the calibration coefficients used. Biases are smaller (or more negative) over land than over sea. This effect mainly disappears when looking at data that are at least 70% clear. This points to some cloud contamination still being present in the CSR. The standard deviations (stdv) of observation minus first guess are about 2-2.5 K which is quite comparable to the values seen for Meteosat–7. The stdv's tend to be higher over land and display a clear diurnal signal there with higher values during day time, the effect again being smaller in the reduced sample of at least 70% clear CSRs.

Figure 26 shows a similar example of timeseries for the IR window channel. The mean bias is about -3 to -3.5 K for all data and about -2. to -2.4 K for 100% clear quadrants. A more detailed investigation had been carried out on the first test data for July 1988 and showed the following characteristics of the IR channel (see also Köpken, 2002). For the 100% clear data, a diurnal cycle with maxima during daytime is visible which corresponds to the diurnal SST cycle (not present in the constant FG SST). The amplitude of this diurnal cycle in OBS-FG may, however, also be due to undetected cloud during night creating cold biases in the nightime CSR data. Note, that this diurnal signal is reversed when looking at all CSR data with differing clear sky fractions. These time series results are comparable to results for Meteosat–7. The stdv shows larger values during day when looking at all CSR data. It is mostly attributed to cloud contaminated data, since this effect is reduced in the 100% clear sample. It does not disappear completely, however, and local skin temperature variations during daytime as well as inaccuracies in the water vapour amount of the model atmosphere may also

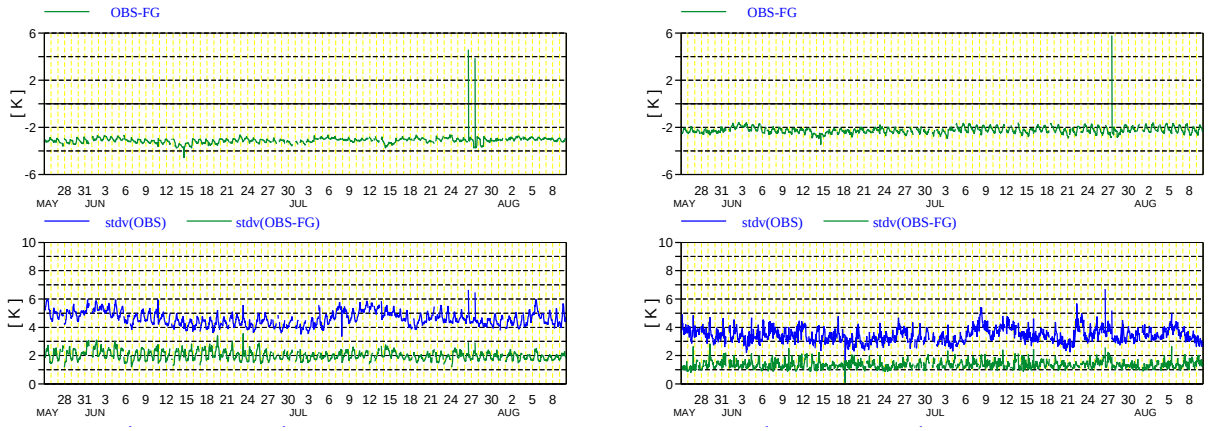

Figure 26: Like Figure 25, but for the IR channel CSR for 27 May to 9 August 1988, all data (left panels) and CSR with a 100% fraction of clear pixels (right panels).

play a role in influencing the standard deviations. Over land there is a strong diurnal cycle in the biases which indicates an underestimation of the model's diurnal land surface temperature amplitudes as was also found in operations when looking at Meteosat–7 data. As for the WV channel, scatter plots for the IR channel indicate that cloud contamination is higher in the Meteosat–2 CSR, as biases versus the model are more negative for quadrants with a low percentage of clear pixels and also occur especially again at cold observed TBs. This effect is stronger over land than over sea, and stronger for Meteosat–2 than for Meteosat–7.

Overall, the quality of the CSR from Meteosat–2 is better than expected giving the more limited bit resolution of the data or the WV and VIS channels. For an assimilation of the WV channel data, two aspects would need to be solved: The first is the setup of quality control thresholds to exclude cloud contaminated observations. Also, the extent of the solar stray light contamination needs to be determined evaluating the monitoring from several years. The second issue is the stability of the vicarious calibration. Since the data are not processed in real-time, a solution may be to first examine time series of the calibration coefficients (available from the processing at EUMETSAT). When this had been done for Meteosat-7 during the period when the vicarious calibration was still used, a good correlation between jumps in these coefficients and jumps in the monitoring time series of the CSR had been found (see Köpken 2001). A smoothing of the calibration coefficients over the reprocessed period and then a 'recalibration' of the CSR radiances with these coefficients may be envisaged to obtain a more stable calibration level for the reprocessed data.

6 Summary and conclusions

During the current fellowship, clear–sky radiance data from Meteosat satellites were monitored in detail and the usage of WV radiances implemented into the operational assimilation. Following the positive results obtained with the Meteosat–7 CSR data, a similar CSR product was initiated in cooperation with CIMSS, and likewise monitored and included into the assimilation. The monitoring of the data allowed demonstration of the improved stability of Meteosat radiances after the introduction of the blackbody calibration, and documention of biases present with respect to the model and other satellites (see Köpken, 2001; Köpken et al., 2002). Current bias estimates for Meteosat–7 are about 3.3 K for the WV channel and -3.5 K for the IR channel, and for Meteosat–5 about 2.5 K for the WV and -4 K for the IR channel. Also, the monitoring allowed description in detail of data specific problems like that caused by the intrusion of solar stray light present in the Meteosat series and the midnight calibration effect visible for the GOES. For assimilation purposes, criteria and periods for the exclusion of these affected data could be set up based on these monitoring results.

The assimilation of WV CSR from the GOES satellites described here confirms the findings made during the experiments using the Meteosat–7 CSR and reported in Köpken et al., 2002. Systematic changes occur, as expected, especially in the upper tropospheric humidity fields and there mainly within the main convergence zones (ITCZ and SPCZ) and adjacent areas. In the ITCZ and SPCZ, humidity is reduced, which is in line with the known model deficiency having a too static ITCZ, while in surrounding areas analyses are on average moister. These changes are in line with departures seen e.g. from HIRS–12, so that the first guess fields are in closer agreement with these observations when the geostationary WV radiances are assimilated. Also with respect to conventional radiosonde humidity observations, a slightly improved first guess fit is noted within the areas of the GOES–8 and GOES–10 disks. Although these results have to be treated with caution given the uncertainty of radiosonde observations at high levels, they do also indicate that the model is overall in better agreement with observations when the geostationary radiances are used. Changes in the wind field do also occur through the time sequence information used in 4DVAR. Small improvements of first guess fit to radiosondes and aircraft (on the southern hemisphere) and American windpropfilers are obtained.

In terms of forecast impact a small positive impact can be seen, both at 500 hPa and at higher levels which again corroborates the positive results found with Meteosat–7 data and led to operational implementation of GOES WV CSR assimilation on 14 January 2003.

Experiments with the new humidity analysis variable developed for the ECMWF analysis, showed that it is efficient in reducing unrealistically high first guess errors occurring in the current system in particularly dry subtropical areas. Also, due to reduced vertical correlations between higher and lower tropospheric levels, currently present humidity increments caused by the WV CSR close to the surface virtually disappear. Therefore, the introduction of this new variable based on a scaled relative humidity is expected to be advantageous also for the assimilation of the geostationary WV CSR.

Concerning the reprocessed CSR data from Meteosat–2, their overall quality is better than expected. This is probably to be attributed to the averaging implied in the derivation of the CSR, which reduces the larger noise present in the pixel data themselves. There seems, however, to be more cloud contamination in the CSR than for the Meteosat–7 data. As for the current Meteosat–5 and –7 satellites, Meteosat–2 is affected by solar stray light effects. Also, the calibration is less stable than for Meteosat–7, since the vicarious calibration based on radiosonde collocations is being used. A surprising finding is that the mean bias versus the model is only about 1 K while the operational satellites have biases of 2.8–3.5 K. The reason for this is currently not understood. An assimilation in future reanalyses may be possible if the calibration can be readjusted to a stable level, e.g. based on the ERA–40 monitoring, and after setting up of suitable data selection criteria excluding remaining cloud contamination and the solar stray light affected time slots.

Future work could include both improving the current usage of the CSR and including additional current and future satellites into active assimilation. With respect to the improvement of the current assimilation, the data selection can be improved upon, e.g. through use of quality criteria in the pre–thinning step (currently applied to used GOES data because of their higher density). Also, quality indicators included with the CSR product could be enhanced, e.g. by using information from the cloud detection scheme used at the satellite processing agency (e.g. including information if thresholds were well or only just satisfied). With the new cloud detection used for MSG (Lutz, 1999) and also implemented for the current Meteosat satellites, such information should be available. Also, evaluation of CSR versus independent cloud information, e.g. obtained from MODIS, can provide additional insights to refine data selection criteria. Finally, once the new humidity analysis is finalized, revisiting the specification of the observation errors in relation to the background errors will be useful.

In addition to using the WV channel, and potentially in the near future the ozone channel of MSG, also the window channel(s) offer additional information. So far it has been used in a diagnostic way to gain a better understanding of model errors of land surface temperature (Köpken et al, 2002; Trigo and Viterbo, 2002). However, the IR channels also contain information on low level humidity which can potentially be used, at least over sea. This would require, though, an accurate SST first guess including the representation of its

diurnal variations as this signal is clearly visible in the observations. Over land, the IR can provide an improved land surface temperature analysis once land surface emissivity is defined more realistically.

Finally, several new satellites will be avilable in future. In early 2003, GOES–9 will replace GMS and enable global coverage with good quality WV radiances, which will be continued through the future MTSAT. The improved GOES–12 will replace the current GOES–8 in April 2003, and MSG with two water vapour channels providing additional information on the vertical structure of the humidity field will be available in 2003. Also the GOES follow–on, ABI, will have additional channels and plans to move sounding from geostationary orbit towards advanced sounders based e.g. on interferometry are underway, like for the planned GIFTS satellite. This will combine the much improved vertical resolution with the high frequency updates possible from geostationary orbit. Also, the much greater amount of spectral information will allow better cloud screening for the selection of clear–sky areas until the assimilation also of cloud affected radiances will become feasible in an operational framework.

Appendix

Satellite monitoring

Figure 27 shows as an example the web page with links to monitoring results for the WV channel of Meteosat–7. Similar pages exist for Meteosat–5, GOES–8, and GOES–10 and will be set up in future for MSG.

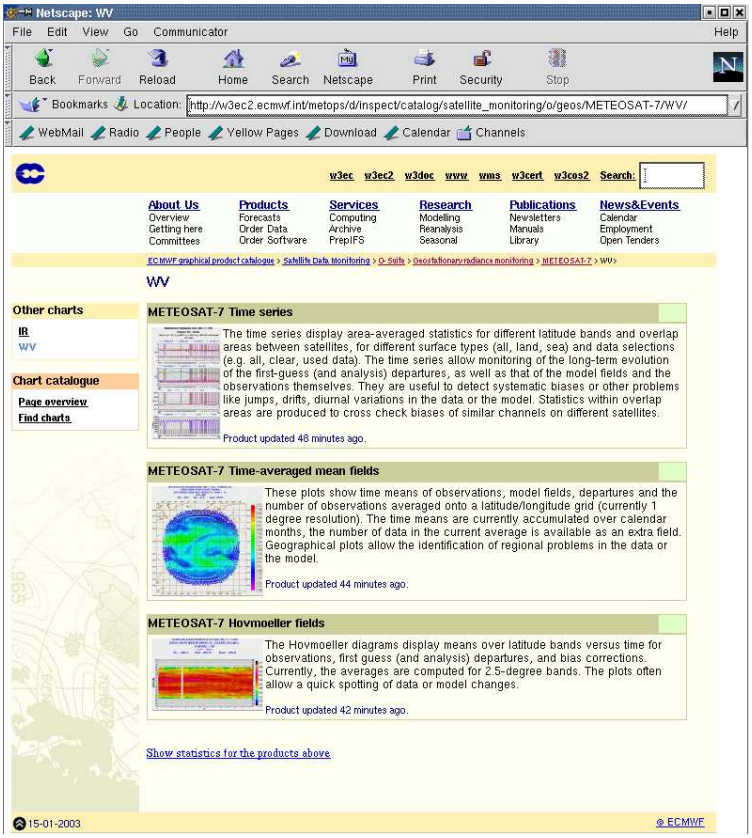

Figure 27: Web page with geostationary satellite data monitoring results in the form of timeseries plots, monthly mean fields on a geographical grid and Latitude mean–time (Hovmoeller) plots. Example for Meteosat–7, WV channel.

Acknowledgements

This work was financed in the framework of the EUMETSAT/ECMWF fellowship programme. The authors would like to thank ECMWF staff, especially E. Andersson, F. Chevallier, A. Simmons, and E. Holm for fruitful discussions during the course of this work. Likewise the technical assistance provided between staff at ECMWF was greatly appreciated and this work benefitted particularly from support by M. Dragosavac in the reception and refining of new data formats for the CSR data, and the experiment system support by J. Haseler and N. Wedi. Graphical support for layout of conference posters was kindly provided by R. Hine. The cooperation with N. Bormann and A. Dethof on the development of satmon, and the help of P. Butterworth for the web–interface was very much enjoyed. Discussions with external colleagues at NCEP (X. Sue, J. Derber) and CMC (L. Garand) provided useful exchanges of experience with geostationary data. Finally, the constructive cooperation with the data providers at EUMETSAT (esp. L. van de Berg, S. Elliot, S. Tjemkes, J. Schmetz, M. K¨onig) and at CIMSS (T. Schmit, T. Schreiner, G. Callan) were very much appreciated. Without their support, the exploitation of these new data would not have been possible.

References

Andersson, E., Pailleux, J., Thépaut, J.-N., Eyre, J. R., McNally, A. P., Kelly, G. A. and Courtier, P., 1994: Use of cloud-cleared radiances in three/four-dimensional variational data assimilation. *Q. J. R. Meteorol. Soc.,***120,** 627-654.

Andersson, E., and H. J¨arvinen, 1999: Variational Quality control. *Q. J. Roy. Met. Soc.*, **125**, 697–722.

Andersson, E., Fisher, M., Munro, R., and McNally, A., 2000: Diagnosis of background errors for observed quantities in a variational 429 data assimilation scheme, and the explanation of a case of poor convergence. *Q. J. R. Meteorol. Soc.,* **126**, 1455–1472.

Derber, J. and F. Bouttier, 1999: A reformulation of the background error covariance in the ECMWF global data assimilation system, Tellus, **51A**, 195-222.

ERA–40, 2001: Proceedings of the workshop on Re–analysis, Reading, 5–9 November 2001. Available from ECMWF, Shinfield Park, Reading, RG2 9AX, U.K.

Holm, E., 2002: Revision of the ECMWF humiity analysis I: Construction of a gaussian control variable. *Proceedings of the ECMWF workshop on humidity analysis*, 8–11 July 2002, ECMWF, Reading, UK.

Holm, E., Andersson, E., Beljaars, A., Lopez, P., Mahfouf, J-F., Simmons, A., and Thpaut, J.-N., 2002: Assimilation and Modelling of the Hydrological Cycle: ECMWF's Status and Plans, *Tech. Memorandum No. 383*. Available from ECMWF, Shinfield Park, Reading, RG2 9AX, U.K.

Johnson, R. X., Weinreb, M., 1996: GOES-8 imager midnight effects and slope correction. *Proceedings of SPIE conference*, 7-9 August 1996, Denver, Colorado, USA.

K¨opken,C. 2001: Monitoring of METEOSAT WV radiances and Solar Stray Light Effects. *EUMETSAT/ECMWF Fellowship Report No. 10*. Available from ECMWF, Shinfield Park, Reading RG2 9AX, UK.

K¨opken, C., 2002: Meteosat–2 Clear–sky radiances: Comments on test data set 1 July – 11 August 1988. Internal note, available from ECMWF, Shinfield Park, Reading RG2 9AX, UK.

K¨opken,C. 2003: Solar stray light effects in Meteosat radiances observed and quantified using operational data monitoring at ECMWF. *J. of Appl. Meteor., in press*.

K¨opken, C., G. Kelly, and J.-N. Thépaut, 2002: Monitoring and assimilation of Meteosat radiances within the 4DVAR system at ECMWF. *EUMETSAT/ECMWF Fellowship Report No. 9*. Available from ECMWF, Shinfield Park, Reading RG2 9AX, UK.

K¨opken, C., G. Kelly, and J.-N. Thépaut, 2003: Assimilation of METEOSAT Radiance Data within the 4DVAR system at ECMWF: Part II. *Q. J. Roy. Met. Soc., in revision*.

Lutz, H.-J., 1999: Cloud processing for Meteosat Second Generation. *Technical Memorandum No. 4*. Available from EUMETSAT, Am Kavallerisand 31, 64295 Darmstadt, Germany.

Macpherson, B., Wright, B. J., Hand, W. H., Maycock, A. J., 1996: The Impact of MOPS Moisture Data in the U.K. Meteorological Office Mesoscale Data Assimilation System.*Mon. Wea. Rev.,***124,** 1746-1766.

McNally, A. P., Derber, J. C., Wu, W. and Katz, B. B., 2000: The use of TOVS level-1b radiances in the NCEP SSI analysis system. *Q. J. R. Meteorol. Soc.,***126,** 689-724.

Munro, R., Kelly, G., Saunders, R., 1999: Assimilation of METEOSAT Radiance Data within the 4DVAR system at ECMWF. *EUMETSAT/ECMWF Fellowship Report No. 8*.

Munro, R., C. K¨opken, G. Kelly, J.-N. Thépaut, and R. Saunders, 2003: Assimilation of METEOSAT Radiance Data within the 4DVAR system at ECMWF: Part I. *Q. J. Roy. Met. Soc., in revision*.

F. Rabier, A. McNally, E. Andersson, P. Courtier, P. Undn, J.R. Eyre, A. Hollingsworth, and F. Bouttier., 1998: The ECMWF implementation of three-dimensional variational assimilation (3D-Var). II: Structure function. *Q. J. Roy. Met. Soc.*, **124B**, 1809-1829.

Trigo, I. and Viterbo, P., 2002: Clear sky window channel radiances: a comparison between observations and the ECMWF model, submitted to J. Appl. Meteor.